Fixed-time formation-containment tracking of heterogeneous multi-agent systems

Shiyu Zhou, Dong Sun, *Fellow, IEEE*, Xiwang Dong, *Senior Member, IEEE*, and Gang Feng*, *Fellow, IEEE*

***Abstract*—In this article, the fixed-time formation-containment tracking (FXFCT) problem is addressed for heterogeneous multi-agent systems (HMASs) under a directed interaction topology. Agents are divided into a reference leader, providing a trajectory for the entire HMASs; formation-leaders, achieving the desired formation by following this trajectory; and followers. Novel distributed fixed-time observers are developed for the formation-leaders and followers with the directed interaction topology, respectively. Distributed fixed-time control protocols are then proposed for the formation-leaders and followers using the coordinate transformation methods, eliminating the restrictive but commonly adopted full-row rank assumption of agent input matrices. It is shown that under the proposed control protocols, the concerned FXFCT problem can be solved. Simulations verify the effectiveness of the obtained theoretical results.**

***Note to Practitioners*—Fixed-time cooperative control of HMASs, e.g., autonomous aerial vehicles (AAVs) and autonomous ground vehicles (AGVs), enables rapid execution of complex collective tasks, efficient resource allocation, and improved operational efficiency. Such capabilities are particularly relevant to applications in logistics, energy management, and smart agriculture, where time-critical coordination delivers significant social and economic benefits. As a unified cooperative control framework, the formation-containment tracking (FCT) problem encompasses several classical problems, such as consensus tracking, formation tracking, and containment control. Solving the FCT problem therefore provides a comprehensive solution that addresses multiple coordination objectives simultaneously, making it particularly relevant for complex real-world missions that require hierarchical coordination in HMASs.**

This paper addresses the FXFCT problem for HMASs under a directed interaction topology. We develop novel distributed fixed-time protocols that integrate distributed fixed-time observers and controllers for both formation-leaders and followers. For practitioners, a key practical advantage lies in an explicit, a priori computable upper bound on the convergence time that is independent of initial conditions, enabling predictable, deadline-aware mission planning. In addition, directed communication and the removal of restrictive full-row rank assumptions on agent dynamics alleviate communication overhead and improve practical applicability to heterogeneous platforms.

***Index Terms*—Fixed-time control, formation-containment tracking, heterogeneous multi-agent systems, cooperative output regulation, directed graph**

This work was supported in part by the Research Grants Council of Hong Kong under project CityU-11205024. The corresponding author is Gang Feng (Tel.: +852 34425900).

Shiyu Zhou and Gang Feng are with the Department of Mechanical Engineering, City University of Hong Kong, Kowloon, Hong Kong SAR, China (e-mail: shiyuzhou9-c@my.cityu.edu.hk (Shiyu Zhou); megfeng@cityu.edu.hk (Gang Feng)).

Dong Sun is with the Department of Biomedical Engineering, City University of Hong Kong, Kowloon, Hong Kong SAR, China (e-mail: medsun@cityu.edu.hk).

Xiwang Dong is with Institute of Unmanned System, School of Artificial Intelligence (Institute of Artificial Intelligence), and School of Automation Science and Electrical Engineering, Science and Technology on Aircraft Control Laboratory, Beihang University, Beijing, 100191, P.R. China (e-mail: xwdong@buaa.edu.cn).

I. Introduction

In recent years, cooperative control of multi-agent systems (MASs), such as consensus, containment, and formation, has drawn considerable attention from various research fields, see, e.g., [1], [2], [3], [4], [5]. Consensus control, a fundamental topic of cooperative control, can generally be divided into leaderless consensus control [6], [7], [8] and leader-following consensus control [9], [10], [11], [12], [13]. In scenarios involving multiple leaders, a typical topic is the so-called containment control problem. The goal of containment control focuses on developing control protocols that allow followers to converge into the convex hull spanned by the leaders. Several related results on this topic have been reported in [14], [15], [16], [17], [18]. However, these existing results typically assume the leaders do not interact or coordinate with each other.

Another typical topic in cooperative control is formation control, whose objective is to steer the entire MAS to form a desired shape. Numerous studies have been reported in the literature addressing the formation control problem, see, for instance, [19], [20], [21], [22], [23]. Several works have further investigated formation-tracking control for first- or second-order MASs [24], [25], homogeneous MASs [26], [27], [28], and heterogeneous MASs [29], [30], [31], in which agents are required to achieve a desired time-varying formation (TVF) while tracking a reference trajectory. When formation objectives are combined with containment requirements, the resulting problem is referred to as formation-containment control. In this setting, leaders are required to achieve a TVF, while followers should converge to the convex hull spanned by the leaders. Recent results on formation-containment control are reported in [32], [33], [34], [35]. In addition to this leader–follower structure, practical applications often require tracking capabilities. Consider, for instance, the air–ground cooperative navigation scenario illustrated in Figure 1, where multiple AAVs serve as formation-leaders, maintaining a TVF while tracking a reference trajectory toward the destination. Meanwhile, AGVs act as followers and are steered to stay within the convex hull formed by the AAVs to ensure coordinated motion and safety during navigation. These requirements motivate the study of FCT, which has received increasing attention (see, e.g., [36], [37], [38]).

It is noted that most of those works mentioned above are based on asymptotic or exponential stability theorems,

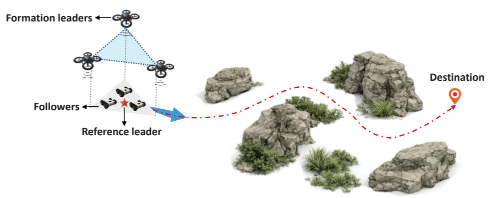

Figure 1. The schematic of air–ground cooperative navigation.

implying that the consensus is only achievable as time approaches infinity. However, these results might not be enough for some practical applications, especially when finite-time ($\mathbf{FIN_t}$) convergence is required. Thus more recently $\mathbf{FIN_t}$ cooperative control of MASs has attracted significant interest [39], [40], [41], [42], [43]. Nevertheless, the upper bound of the convergence time for $\mathbf{FIN_t}$ cooperative control in [39], [40], [41] depends on the initial states of agents and could grow unbounded as the initial state moves further from the equilibrium point. To address this limitation of $\mathbf{FIN_t}$ convergence, the concept of fixed-time ($\mathbf{FIX_t}$) convergence was first introduced in [44], which allows the convergence time to be upper bounded by a constant independent of the initial conditions. Following this concept, some effort has been devoted to the $\mathbf{FIX_t}$ cooperative control problems, see, for example, [45], [46], [47], [48], [49], [50], [51]. In particular, the FXFCT control problem for HMASs was investigated in [51], where the interaction topology was assumed to be undirected and a restrictive full-row rank assumption concerning the input matrices of the followers was implicitly required. In fact, to the best of our knowledge, the FXFCT control problem of HMASs under directed interaction topologies without the restrictive assumption is still open, which motivates this study. The main contributions of this work are three folds:

1) Unlike [48], [49], [50], [51] where the $\mathbf{FIX_t}$ cooperative control problems with *undirected or strongly connected interaction topologies* are considered, more general HMASs with a *directed interaction topology* are studied in this work. Noting that the Laplacian matrix of the directed graph is asymmetric, novel distributed $\mathbf{FIX_t}$ observers and stability analysis methods are developed in this work. It is shown that the proposed methodology is effective in dealing with the directed graph to achieve the desired FXFCT.
2) Different from the existing FXFCT control scheme for HMASs [51], which implicitly imposes the full-row rank condition on the input matrices of the agents, this work eliminates this restrictive assumption by designing novel $\mathbf{FIX_t}$ formation-tracking and containment protocols based on coordinate transformation methods.
3) In contrast with the works on $\mathbf{FIX_t}$ formation tracking control or containment control of MASs [46], [47], [50], the FXFCT control problem is more challenging, as it requires formation-leaders and followers to achieve both formation tracking and containment in a fixed time simultaneously.

Notation: Let I_n be the n-dimensional identity matrix and $\otimes$ represent the Kronecker product. A diagonal matrix with diagonal entries $k_1, \ldots, k_n$ is denoted by $\mathrm{diag}\{k_1, \ldots, k_n\}$. $\|\cdot\|$ and $\|\cdot\|_q$ represent the Euclidean norm and q-norm of vectors, respectively. Given a vector $\mathcal{A} = [a_1, \ldots, a_n]^\top \in \mathbb{R}^n$, define $\mathrm{sign}^c(\mathcal{A}) = [\mathrm{sign}(a_1)|a_1|^c, \ldots, \mathrm{sign}(a_n)|a_n|^c]^\top$, where $c > 0$ and $\mathrm{sign}(\cdot)$ stands for the sign function. The distance from $\mathcal{A}$ to set $\mathcal{S}$ is denoted by $\mathrm{dist}(\mathcal{A}, \mathcal{S}) = \inf_{x\in\mathcal{S}} \|\mathcal{A} - x\|$. The operators $\min(\cdot)$ and $\max(\cdot)$ are used to obtain the smallest and largest elements of an array, respectively. For a finite point set $P = \{p_1, \ldots, p_n\}$, its convex hull is defined as $\mathrm{Co}(P) = \{\sum_{i=1}^n l_i p_i | p_i \in P, l_i \in \mathbb{R}, l_i \geq 0, \sum_{i=1}^n l_i = 1\}$.

II. Preliminaries and Problem formulation

A. Preliminaries

Let $\mathcal{G} = (\mathcal{O}, \mathcal{E}, \Omega)$ represent the digraph among the MAS under consideration, with the set of nodes $\mathcal{O} = \{1, \cdots, m\}$, the set of edges $\mathcal{E} \subseteq \mathcal{O} \times \mathcal{O}$, and the weighted adjacency matrix $\Omega = [\omega_{ij}]_{m\times m}$ with $\omega_{ij} > 0 \Leftrightarrow (j, i) \in \mathcal{E}$ and $\omega_{ij} = 0$ otherwise. A spanning tree is a digraph in which at least one root node has a directed path to all other nodes. The Laplacian matrix $\mathcal{L} = [l_{ij}]_{m\times m}$ associated with digraph $\mathcal{G}$ is defined by $l_{ij} = -\omega_{ij}$, $i \neq j$, and $l_{ij} = \sum_{j=1}^m \omega_{ij}$. Let $\mathcal{N}_i = \{j \in \mathcal{O} | (j, i) \in \mathcal{E}\}$ denote the set of neighbors of agent i.

B. Problem formulation

In this paper, we consider a HMAS with M formation-leaders and N followers whose dynamics are described by:

$$\begin{aligned} &\dot{x}_i(t) = A_i x_i(t) + B_i u_i(t), \\ &y_i(t) = C_i x_i(t),\ i = 1, \ldots, M+N, \end{aligned} \tag{1}$$

where $x_i \in \mathbb{R}^{n_i}$, $u_i \in \mathbb{R}^{m_i}$, $y_i \in \mathbb{R}^p$ represent the state, control input, and output of the i-th agent, respectively, A_i, B_i, and C_i are the system matrices of agent i satisfying $\mathrm{rank}(B_i) = m_i$.

The dynamics of the reference leader are described by:

$$\begin{aligned} &\dot{x}_0(t) = A_0 x_0(t), \\ &y_0(t) = C_0 x_0(t), \end{aligned} \tag{2}$$

where $x_0 \in \mathbb{R}^{n_0}$ and $y_0 \in \mathbb{R}^p$ represent the state and output of the reference leader, A_0 and C_0 are the system matrices of the reference leader.

According to [36], [37], within the framework of FCT control, the agents are categorized into three types based on their specific roles and task requirements: the reference leader, formation-leaders, and followers. The reference leader is responsible for providing a reference trajectory for the MAS under consideration. The formation-leaders, whose neighbors are only leaders, are tasked with forming a TVF while simultaneously tracking the trajectory provided by the reference leader. The followers are required to converge to the convex hull spanned by the formation-leaders.

Let $\mathcal{O}_{fl} = \{1, \ldots, M\}$ and $\mathcal{O}_f = \{\bar{N}_1, \ldots, \bar{N}_N\}$ with $\bar{N}_i = M + i$ for $i = 1, \ldots, N$ be the sets of the formation-leaders and followers, respectively. The Laplacian matrix can be written as follows,

$$\mathcal{L} = \begin{pmatrix} 0 & 0_{1\times M} & 0_{1\times N} \\ \mathcal{L}_L & \mathcal{L}_{FL} & 0_{M\times N} \\ 0_{N\times 1} & \mathcal{L}_{FF} & \mathcal{L}_F \end{pmatrix}, \tag{3}$$

where $\mathcal{L}_L \in \mathbb{R}^{M\times 1}$, $\mathcal{L}_{FL} \in \mathbb{R}^{M\times M}$, $\mathcal{L}_{FF} \in \mathbb{R}^{N\times M}$, and $\mathcal{L}_F \in \mathbb{R}^{N\times N}$.

The piecewise continuous differentiable TVF vector $h_{yi}(t) \in \mathbb{R}^p$ is generated through the system given by

$$\begin{aligned} \dot{h}_{xi}(t) &= A_h h_{xi}(t), \\ h_{yi}(t) &= C_h h_{xi}(t),\ i \in \mathcal{O}_{fl}, \end{aligned} \tag{4}$$

where $h_{xi} \in \mathbb{R}^l$, A_h and C_h are matrices with compatible dimensions.

Remark 1. *In* (4)*, $h_{xi}(t)$ is an auxiliary state used to generate the desired formation vector, while $h_{yi}(t) = C_h h_{xi}(t)$ denotes the corresponding desired output formation vector. Specifically, for each formation-leader, $h_{yi}(t)$ describes its relative offset with respect to the reference output $y_0(t)$. By properly choosing A_h and C_h, equation* (4) *can describe different formation patterns, such as time-invariant and rotating formations; see, e.g., [26], [38].*

This paper aims to address the problem as formulated below.

Definition 1 (Fixed-time formation-containment tracking (FXFCT) problem)**.** *Given the HMAS consisting of (1) and (2) under a digraph, find a distributed control protocol for each formation-leader such that*

$$\lim_{t\to T} \left(y_i(t) - h_{yi}(t) - y_0(t)\right) = 0,\ \forall i \in \mathcal{O}_{fl}, \tag{5}$$

and a distributed control protocol for each follower such that

$$\lim_{t\to T} \operatorname{dist}\left(y_i(t), \operatorname{Co}(y_j(t), j \in \mathcal{O}_{fl})\right) = 0,\ \forall i \in \mathcal{O}_f, \tag{6}$$

where $T > 0$ denotes the convergence time that is independent of the initial states of the concerned MAS.

III. Main Results

This section presents the main results of this paper. To proceed, the following assumptions are put forward.

Assumption 1. *The reference leader is globally reachable to formation-leaders in the interaction topology.*

Assumption 2. *For each follower, there is at least one directed path from one formation-leader.*

Under Assumptions 1 and 2, the following two technical lemmas can be obtained.

Lemma 1 ([6])**.** *Under Assumptions 1 and 2, all eigenvalues of $\mathcal{L}_{FL}$ and $\mathcal{L}_F$ have positive real parts, $-\mathcal{L}_F^{-1}\mathcal{L}_{FF}$ is nonnegative, and $-\mathcal{L}_F^{-1}\mathcal{L}_{FF}\mathbf{1}_M = \mathbf{1}_N$.*

Lemma 2 ([52])**.** *Under Assumptions 1 and 2, there exists positive diagonal matrices $\bar{G}_{FL}$ and $\bar{G}_F$, such that $\bar{G}_{FL}\mathcal{L}_{FL} + \mathcal{L}_{FL}^\top \bar{G}_{FL} > 0$ and $\bar{G}_F\mathcal{L}_F + \mathcal{L}_F^\top \bar{G}_F > 0$.*

Let $\lambda_{FL,\min} > 0$ and $\lambda_{F,\min} > 0$ be the smallest eigenvalue of $\bar{G}_{FL}\mathcal{L}_{FL} + \mathcal{L}_{FL}^\top \bar{G}_{FL} > 0$ and $\bar{G}_F\mathcal{L}_F + \mathcal{L}_F^\top \bar{G}_F > 0$, respectively. Moreover, define $G_{FL} = \operatorname{diag}\{g_{fl_1}, \ldots, g_{fl_M}\} := \frac{2\bar{G}_{FL}}{\lambda_{FL,\min}}$ and $G_F = \operatorname{diag}\{g_{f_1}, \ldots, g_{f_N}\} := \frac{2\bar{G}_F}{\lambda_{F,\min}}$, where $g_{fl_i} > 0$, $i \in \mathcal{O}_{fl}$, and $g_{f_j} > 0$, $j \in \mathcal{O}_f$. Then, via Lemma 2, one has $G_{FL}\mathcal{L}_{FL} + \mathcal{L}_{FL}^\top G_{FL} \geq 2\mathrm{I}_M$ and $G_F\mathcal{L}_F + \mathcal{L}_F^\top G_F \geq 2\mathrm{I}_N$.

In addition, the following standard assumptions are also made.

Assumption 3. *For any $i \in \mathcal{O}_f \cup \mathcal{O}_{fl}$, (A_i, B_i) are controllable.*

Assumption 4. *The regulator equations,*

$$\Xi_i A_0 = A_i \Xi_i + B_i \Gamma_i \tag{7a}$$
$$0 = C_i \Xi_i - C_0, \tag{7b}$$

have solution pairs (Ξ_i, Γ_i) for all $i \in \mathcal{O}_f \cup \mathcal{O}_{fl}$.

Assumption 5. *The linear matrix equations,*

$$\Xi_{hi} A_h = A_i \Xi_{hi} + B_i \Gamma_{hi}, \tag{8a}$$
$$0 = C_i \Xi_{hi} - C_h, \tag{8b}$$

have solution pairs (Ξ_{hi}, Γ_{hi}) for all $i \in \mathcal{O}_f \cup \mathcal{O}_{fl}$.

Remark 2. *Assumptions 4-5 are necessary for achieving the FCT as in [36], [37], [51]. As detailed in [53], the regulator equations (7) can be solved if* $\operatorname{rank}\begin{bmatrix} A_i - \lambda I_{n_i} & B_i \\ C_i & 0 \end{bmatrix} = n_i + p$ *holds for all $\lambda \in \sigma(A_0)$, where $\sigma(A_0)$ represents the spectrum of A_0.*

A. $\mathbf{FIX_t}$ *formation tracking control of formation-leaders*

The distributed $\mathbf{FIX_t}$ formation tracking control protocol is designed as follows,

$$u_i = \Gamma_i \eta_i + \Gamma_{hi} h_{xi} + z_i, \tag{9a}$$
$$\dot{\eta}_i = A_0 \eta_i - \mu_1 \theta_i - \mu_2 \operatorname{sign}^{\alpha_1}(\theta_i) - \mu_3 \operatorname{sign}^{\alpha_2}(\theta_i), i \in \mathcal{O}_{fl}, \tag{9b}$$

where $\theta_i = \sum_{j=1}^M \omega_{ij}(\eta_i - \eta_j) + \omega_{i0}(\eta_i - x_0)$, η_i is the state of the observer, θ_i denotes the neighboring relative estimation error, and the parameters μ_1, μ_2, μ_3, α_1, α_2 are positive constants that will be decided later, Γ_i and Γ_{hi} are the solutions to equations (7) and (8) respectively, and z_i will be determined later for achieving $\mathbf{FIX_t}$ formation tracking.

Given that not all formation-leaders have access to the state of the reference leader, the distributed $\mathbf{FIX_t}$ observer (9b) is proposed to estimate x_0. Define the estimation error $\tilde{\eta}_i = \eta_i - x_0$, $i \in \mathcal{O}_{fl}$. Then, we will present the following lemma on the distributed $\mathbf{FIX_t}$ observer (9b).

Lemma 3. *Consider the distributed $\mathbf{FIX_t}$ observer (9b). Let μ_1, μ_2, μ_3, α_1, and α_2, be chosen such that $\mu_1 > \|G_{FL} \otimes A_0\|$, $\mu_2 > 0$, $\mu_3 > 0$, $0 < \alpha_1 < 1$, $\alpha_2 > \frac{1}{\alpha_1} > 1$. There is a settling time $T_\eta \geq 0$ regardless of any initial conditions, such that $\lim_{t\to T_\eta} \tilde{\eta}_i(t) = 0$ and $\tilde{\eta}_i(t) = 0$, $t \geq T_\eta$, $\forall i \in \mathcal{O}_{fl}$.*

Proof. Letting $\tilde{\eta} = [\tilde{\eta}_1^\top, \ldots, \tilde{\eta}_M^\top]^\top$ and $\bar{\theta} = \left[\bar{\theta}_1^\top, \ldots, \bar{\theta}_M^\top\right]^\top$ with $\bar{\theta}_i = \mu_1\theta_i + \mu_2 \operatorname{sign}^{\alpha_1}(\theta_i) + \mu_3 \operatorname{sign}^{\alpha_2}(\theta_i)$, it follows from (2) and (9b) that

$$\dot{\tilde{\eta}} = (\mathrm{I}_M \otimes A_0)\,\tilde{\eta} - (\mathrm{I}_M \otimes \mathrm{I}_{n_0})\,\bar{\theta}. \tag{10}$$

Let $\theta = [\theta_1^\top, \ldots, \theta_M^\top]^\top$. Noting that $\theta = (\mathcal{L}_{FL} \otimes \mathrm{I}_{n_0})\tilde{\eta}$, it then follows from (10) that

$$\dot{\theta} = (I_M \otimes A_0)\,\theta - (\mathcal{L}_{FL} \otimes \mathrm{I}_{n_0})\,\bar{\theta}. \tag{11}$$

Consider the Lyapunov function candidate,

$$V_1 = \sum_{i=1}^{M}\left(\frac{\mu_2 g_{fl_i}}{1+\alpha_1}\|\theta_i\|_{1+\alpha_1}^{1+\alpha_1} + \frac{\mu_3 g_{fl_i}}{1+\alpha_2}\|\theta_i\|_{1+\alpha_2}^{1+\alpha_2}\right) + \frac{\mu_1}{2}\theta^\top(G_{FL}\otimes \mathrm{I}_{n_0})\theta. \tag{12}$$

The time derivative of (12) along (11) satisfies

$$\dot{V}_1 = \bar{\theta}^\top(G_{FL}\otimes A_0)\theta - \frac{1}{2}\bar{\theta}^\top\left(\Delta_{FL}\otimes I_{n_0}\right)\bar{\theta}, \tag{13}$$

where $\Delta_{FL} \triangleq G_{FL}\mathcal{L}_{FL} + \mathcal{L}_{FL}^\top G_{FL} \geq 2\mathrm{I}_M$. Via Young's inequality, one has $\bar{\theta}^\top(G_{FL}\otimes A_0)\theta \leq \frac{\|G_{FL}\otimes A_0\|^2}{2}\|\theta\|^2 + \frac{1}{2}\|\bar{\theta}\|^2$. Then, one has

$$\dot{V}_1 \leq \frac{1}{2}(\|G_{FL}\otimes A_0\|^2\|\theta\|^2 - \|\bar{\theta}\|^2). \tag{14}$$

Note that $\bar{\theta} = [\bar{\theta}_1^\top,\ldots,\bar{\theta}_M^\top]^\top$, where $\bar{\theta}_i = \mu_1\theta_i + \mu_2\mathrm{sign}^{\alpha_1}(\theta_i) + \mu_3\mathrm{sign}^{\alpha_2}(\theta_i)$. Since $\mu_j > 0$, $j=1,2,3$, the corresponding components of θ_i, $\mathrm{sign}^{\alpha_1}(\theta_i)$, and $\mathrm{sign}^{\alpha_2}(\theta_i)$ have the same sign. Therefore, the inner-product terms appearing in the expansion of $\|\bar{\theta}_i\|^2$ are nonnegative. Then, one has $\|\bar{\theta}\|^2 = \sum_{i=1}^M\|\bar{\theta}_i\|^2 \geq \sum_{i=1}^M \mu_1^2\|\theta_i\|^2 + \sum_{i=1}^M \mu_2^2\|\theta_i\|_{2\alpha_1}^{2\alpha_1} + \sum_{i=1}^M \mu_3^2\|\theta_i\|_{2\alpha_2}^{2\alpha_2}$. Since $0<\alpha_1<1$ and $\alpha_2>1$, by Lemma 6 given in Appendix, one has $\sum_{i=1}^M\|\theta_i\|_{2\alpha_1}^{2\alpha_1} \geq \left(\|\theta\|^2\right)^{\alpha_1}$ and $\sum_{i=1}^M\|\theta_i\|_{2\alpha_2}^{2\alpha_2} \geq \frac{1}{(n_0M)^{\alpha_2-1}}\left(\|\theta\|^2\right)^{\alpha_2}$. Then, one can obtain that

$$\|\bar{\theta}\|^2 \geq \mu_1^2\|\theta\|^2 + \mu_2^2\left(\|\theta\|^2\right)^{\alpha_1} + \frac{\mu_3^2\left(\|\theta\|^2\right)^{\alpha_2}}{(n_0M)^{\alpha_2-1}}. \tag{15}$$

Substituting (15) into (14) yields

$$\dot{V}_1 \leq -c_\theta\left(\|\theta\|^2 + \left(\|\theta\|^2\right)^{\alpha_1} + \left(\|\theta\|^2\right)^{\alpha_2}\right), \tag{16}$$

where $c_\theta = \min\left\{\frac{\mu_1^2 - \|G_{FL}\otimes A_0\|^2}{2}, \frac{\mu_2^2}{2}, \frac{\mu_3^2}{2(n_0M)^{\alpha_2-1}}\right\} > 0$.

Since $0<\alpha_1<1$ and $\alpha_2>1$, via Lemma 6, one has $\sum_{i=1}^M\frac{\mu_2 g_{fl_i}}{1+\alpha_1}\|\theta_i\|_{1+\alpha_1}^{1+\alpha_1} \leq \bar{\mu}_2(\|\theta\|^2)^{\frac{1+\alpha_1}{2}}$ and $\sum_{i=1}^M\frac{\mu_3 g_{fl_i}}{1+\alpha_2}\|\theta_i\|_{1+\alpha_2}^{1+\alpha_2} \leq \bar{\mu}_3(\|\theta\|^2)^{\frac{1+\alpha_2}{2}}$, where $\bar{\mu}_2 = (\frac{\mu_2 g_{fl,\max}}{1+\alpha_1})(n_0M)^{\frac{1-\alpha_1}{2}}$, $\bar{\mu}_3 = \frac{\mu_3 g_{fl,\max}}{1+\alpha_2}$, and $g_{fl,\max} = \max\{g_{fl_1},\ldots,g_{fl_M}\}$. Noting that $0 < \frac{2\alpha_1}{1+\alpha_1} < 1$ and $\frac{2\alpha_2}{1+\alpha_2} > 1$, via Lemma 6 and (12), one can obtain that

$$V_1^{\frac{2\alpha_1}{1+\alpha_1}} \leq c_{\alpha_1}\left((\|\theta\|^2)^{\frac{2\alpha_1}{1+\alpha_1}} + (\|\theta\|^2)^{\alpha_1} + (\|\theta\|^2)^{\frac{\alpha_1(1+\alpha_2)}{1+\alpha_1}}\right), \tag{17}$$

and

$$V_1^{\frac{2\alpha_2}{1+\alpha_2}} \leq c_{\alpha_2}\left((\|\theta\|^2)^{\frac{2\alpha_2}{1+\alpha_2}} + (\|\theta\|^2)^{\frac{\alpha_2(1+\alpha_1)}{1+\alpha_2}} + (\|\theta\|^2)^{\alpha_2}\right), \tag{18}$$

where $c_{\alpha_1} = \max\{(\frac{\mu_1 g_{fl,\max}}{2})^{\frac{2\alpha_1}{1+\alpha_1}}, \bar{\mu}_2^{\frac{2\alpha_1}{1+\alpha_1}}, \bar{\mu}_3^{\frac{2\alpha_1}{1+\alpha_1}}\}$ and $c_{\alpha_2} = \max\{(\frac{\mu_1 g_{fl,\max}}{2})^{\frac{2\alpha_2}{1+\alpha_2}}, \bar{\mu}_2^{\frac{2\alpha_2}{1+\alpha_2}}, \bar{\mu}_3^{\frac{2\alpha_2}{1+\alpha_2}}\} \times 3^{\frac{\alpha_2-1}{\alpha_2+1}}$. Noting that $\alpha_1 < \frac{2\alpha_1}{1+\alpha_1} < 1$ and $\alpha_1 < \frac{\alpha_1(1+\alpha_2)}{1+\alpha_1} < \alpha_2$, one has $(\|\theta\|^2)^{\frac{2\alpha_1}{1+\alpha_1}} \leq \|\theta\|^2 + (\|\theta\|^2)^{\alpha_1}$ and $(\|\theta\|^2)^{\frac{\alpha_1(1+\alpha_2)}{1+\alpha_1}} \leq (\|\theta\|^2)^{\alpha_1} + (\|\theta\|^2)^{\alpha_2}$. Similarly, since $1 < \frac{2\alpha_2}{1+\alpha_2} < \alpha_2$ and $\alpha_1 < \frac{\alpha_2(1+\alpha_1)}{1+\alpha_2} < \alpha_2$, one can obtain that $(\|\theta\|^2)^{\frac{2\alpha_2}{1+\alpha_2}} \leq \|\theta\|^2 + (\|\theta\|^2)^{\alpha_2}$ and $(\|\theta\|^2)^{\frac{\alpha_2(1+\alpha_1)}{1+\alpha_2}} \leq (\|\theta\|^2)^{\alpha_1} + (\|\theta\|^2)^{\alpha_2}$. Then, one can obtain that

$$V_1^{\frac{2\alpha_1}{1+\alpha_1}} \leq c_{\alpha_1}\left(\|\theta\|^2 + 3(\|\theta\|^2)^{\alpha_1} + (\|\theta\|^2)^{\alpha_2}\right), \tag{19}$$

and

$$V_1^{\frac{2\alpha_2}{1+\alpha_2}} \leq c_{\alpha_2}\left(\|\theta\|^2 + 3(\|\theta\|^2)^{\alpha_2} + (\|\theta\|^2)^{\alpha_1}\right). \tag{20}$$

Combining (19) and (20), one has

$$\frac{V_1^{\frac{2\alpha_1}{1+\alpha_1}}}{4c_{\alpha_1}} + \frac{V_1^{\frac{2\alpha_2}{1+\alpha_2}}}{4c_{\alpha_2}} \leq \|\theta\|^2 + (\|\theta\|^2)^{\alpha_2} + (\|\theta\|^2)^{\alpha_1}. \tag{21}$$

Substituting (21) into (16), one has

$$\dot{V}_1 \leq -\frac{c_\theta}{4c_{\alpha_1}}V_1^{\frac{2\alpha_1}{1+\alpha_1}} - \frac{c_\theta}{4c_{\alpha_2}}V_1^{\frac{2\alpha_2}{1+\alpha_2}}. \tag{22}$$

By Lemma 7 in Appendix and (22), it can be shown that system (11) is $\mathbf{FIX_t}$ stable. The associated settling time satisfies $T_\eta \leq \frac{4c_{\alpha_1}(1+\alpha_1)}{c_\theta(1-\alpha_1)} + \frac{4c_{\alpha_2}(1+\alpha_2)}{c_\theta(\alpha_2-1)}$. Moreover, since $\theta(t) = (\mathcal{L}_{FL}\otimes \mathrm{I}_{n_0})\tilde{\eta}(t)$ and $\mathcal{L}_{FL}$ is nonsingular, we have $\lim_{t\to T_\eta}\tilde{\eta}_i(t) = 0$ and $\tilde{\eta}_i(t) = 0$ for $t \geq T_\eta$. Thus, the proof is completed. □

Then, we proceed to design the $\mathbf{FIX_t}$ formation tracking control component z_i in (9a). Define $\hat{e}_{fl,i} = x_i - \Xi_i\eta_i - \Xi_{hi}h_{xi}$, $i \in \mathcal{O}_{fl}$. Given that (A_i, B_i) is controllable and $\mathrm{rank}(B_i) = m_i$, via Lemma 8 given in Appendix, there exists a linear coordinate transformation $\hat{\zeta}_i = T_i\hat{e}_{fl,i} = \left[\hat{\zeta}_{i1,1},\ldots,\hat{\zeta}_{i1,\rho_1},\ldots,\ \hat{\zeta}_{im_i,1},\ldots,\hat{\zeta}_{im_i,\rho_{m_i}}\right]^\top$, where ρ_j, $j = 1,\ldots,m_i$, denotes the controllability index of $\hat{\zeta}_{ij}$. Then, z_i is proposed as follows,

$$z_i = M_i^{-1}(w_i - D_i\hat{e}_{fl,i}), \tag{23}$$

where $w_i = [w_{i1},\ldots,w_{ij},\ldots,w_{im_i}]^\top$ with $w_{ij} = -\sum_{k=1}^{\rho_j}\left(c_{ij,k}\mathrm{sign}^{p_{ij,k}}(\hat{\zeta}_{ij,k}) + \bar{c}_{ij,k}\mathrm{sign}^{\bar{p}_{ij,k}}(\hat{\zeta}_{ij,k})\right)$, D_i and invertible matrix M_i are designed as in Lemma 8, $c_{ij,k}$, $\bar{c}_{ij,k}$, $p_{ij,k}$, and $\bar{p}_{ij,k}$, $j=1,\ldots,m_i$, $k=1,\ldots,\rho_j$, are chosen according to Lemma 9 in Appendix.

Then, the main result of this subsection is presented as follows.

Theorem 1. *Let Assumptions 1-5 be satisfied. Consider the reference leader (2) and M formation-leaders (1). The $\mathbf{FIX_t}$ formation tracking problem described by (5) is solved under the protocols defined in (9) and (23).*

Proof. The proof of Theorem 1 includes two steps. Firstly, the formation tracking errors are proved to be bounded in $[0, T_\eta)$, ensuring that no $\mathbf{FIN_t}$ escape occurs. Then, the formation tracking errors are proved to converge to zero in a fixed time.

Step 1: Under Assumptions 4 and 5, one can obtain from (1), (4), and (9) that

$$\dot{\hat{e}}_{fl,i} = A_i\hat{e}_{fl,i} + B_iz_i + \Xi_i\bar{\theta}_i. \tag{24}$$

Note that $\hat{\zeta}_i = T_i\hat{e}_{fl,i} = [\hat{\zeta}_{i1,1},\ldots,\hat{\zeta}_{i1,\rho_1},\ldots,\hat{\zeta}_{im_i,1},\ldots,\hat{\zeta}_{im_i,\rho_{m_i}}]^\top$. Letting $\Delta_i = T_i\Xi_i\bar{\theta}_i = [\Delta_{i1,1},\ldots,\Delta_{i1,\rho_1},\ldots,\Delta_{im_i,1},\ldots,\Delta_{im_i,\rho_{m_i}}]^\top$, via (23), the dynamics of $\hat{\zeta}_{ij}$, $j=1,\ldots,m_i$, has the following form,

$$\begin{cases} \dot{\hat{\zeta}}_{ij,1} = \hat{\zeta}_{ij,2} + \Delta_{ij,1}, \\ \dot{\hat{\zeta}}_{ij,2} = \hat{\zeta}_{ij,3} + \Delta_{ij,2}, \\ \quad\vdots \\ \dot{\hat{\zeta}}_{ij,\rho_j} = w_{ij} + \Delta_{ij,\rho_j}, \end{cases} \tag{25}$$

where $w_{ij} = -\sum_{k=1}^{\rho_j} \left(c_{ij,k}\mathrm{sign}^{p_{ij,k}}(\hat{\zeta}_{ij,k}) + \bar{c}_{ij,k}\mathrm{sign}^{\bar{p}_{ij,k}}(\hat{\zeta}_{ij,k}) \right)$.

It is established in [54] that system (25) is bounded-input-bounded-state (BIBS) stable when $\Delta_{ij} = [\Delta_{ij,1}, \ldots, \Delta_{ij,\rho_j}]^\top$ is regarded as the input. According to Lemma 3, $\bar{\theta}_i$ is bounded in $[0, T_\eta)$, and therefore Δ_{ij}, $j = 1, \ldots, m_i$, are bounded on the same interval. As a result, $\hat{\zeta}_i$ remains bounded as well. Since $\hat{\zeta}_i = T_i \hat{e}_{fl,i}$ and T_i is nonsingular, it follows that $\hat{e}_{fl,i}$ is bounded in $[0, T_\eta)$.

Step 2: From Lemma 3, one has $\eta_i(t) = x_0(t)$ for $t \geq T_\eta$, which implies that $\hat{e}_{fl,i} = e_{fl,i} = x_i - \Xi_i x_0 - \Xi_{hi} h_{xi}$ and $\Delta_i = 0$.

Via Lemma 9, it follows that system (25) is $\mathbf{FIX_t}$ stable for all $j \in \{1, \ldots, m_i\}$. The corresponding settling time satisfies $T_{fl} \leq T_\eta + T_\zeta$, with T_η and T_ζ defined by Lemma 3 and Lemma 9, respectively. Given that $\zeta_i = T_i e_{fl,i}$, where T_i is invertible, and $e_{Li} = C_i e_{fl,i} = y_i - h_{yi} - y_0$, it is concluded that $\lim_{t\to T_{fl}} e_{Li}(t) = 0$ and $e_{Li}(t) = 0$ for $t \geq T_{fl}$. □

B. $\mathbf{FIX_t}$ *containment control of followers*

The distributed $\mathbf{FIX_t}$ containment control protocol is designed as follows,

$$u_i = \Gamma_i \sigma_i + \Gamma_{hi}\phi_i + v_i, \tag{26a}$$
$$\dot{\sigma}_i = A_0\sigma_i - \vartheta_1 \varsigma_i - \vartheta_2 \mathrm{sign}^{\beta_1}(\varsigma_i) - \vartheta_3 \mathrm{sign}^{\beta_2}(\varsigma_i), \tag{26b}$$
$$\dot{\phi}_i = A_h\phi_i - \imath_1\varphi_i - \imath_2\mathrm{sign}^{\gamma_1}(\varphi_i) - \imath_3\mathrm{sign}^{\gamma_2}(\varphi_i), i \in \mathcal{O}_f, \tag{26c}$$

where $\varsigma_i = \sum_{j=M+1}^{M+N} \omega_{ij}(\sigma_i - \sigma_j) + \sum_{j=1}^{M} \omega_{ij}(\sigma_i - \eta_j)$, $\varphi_i = \sum_{j=M+1}^{M+N} \omega_{ij}(\phi_i - \phi_j) + \sum_{j=1}^{M} \omega_{ij}(\phi_i - h_{xj})$, σ_i represents the state of the $\mathbf{FIX_t}$ distributed observer used to estimate x_0 via the information η_j, ϕ_i denotes the state of the distributed observer to estimate $\mathrm{Co}(h_{xj}(t), j \in \mathcal{O}_{fl})$, the parameters ϑ_1, ϑ_2, ϑ_3, $\imath_1$, $\imath_2$, $\imath_3$, β_1, β_2, γ_1, and γ_2 are positive constants that will be decided later, Γ_i and Γ_{hi} are the solutions to equations (7) and (8) respectively, and v_i will be determined later for achieving $\mathbf{FIX_t}$ containment.

Given that the followers cannot access the state x_0, the distributed $\mathbf{FIX_t}$ observer (26b) is proposed to estimate x_0 through the information η_j in (9b). Additionally, as the TVF vector h_{xj}, $j \in \mathcal{O}_{fl}$, is accessible only to part of the followers, the distributed $\mathbf{FIX_t}$ observer (26c) is proposed to estimate $\mathrm{Co}(h_{xj}(t), j \in \mathcal{O}_{fl})$. Define the estimation error $\tilde{\sigma}_i = \sigma_i - x_0$, $i \in \mathcal{O}_f$. We present several technical lemmas related to these distributed observers (26b) and (26c) as follows.

Lemma 4. *Suppose Assumptions 1 and 2 hold. Consider the reference leader (2), the distributed observer (9b), and the distributed observer (26b). Let ϑ_1, ϑ_2, ϑ_3, β_1, and β_2, be chosen such that $\vartheta_1 > \|G_F \otimes A_0\|$, $\vartheta_2 > 0$, $\vartheta_3 > 0$, $0 < \beta_1 < 1$, $\beta_2 > \frac{1}{\beta_1} > 1$. There is a settling time $T_\sigma \geq 0$ regardless of any initial conditions, such that $\lim_{t\to T_\sigma} \tilde{\sigma}_i(t) = 0$ and $\tilde{\sigma}_i(t) = 0,\ t \geq T_\sigma,\ \forall i \in \mathcal{O}_f$.*

Proof. The proof is to be accomplished via the following two steps.

Step 1: Boundedness of σ_i in $t \in [0, T_\eta)$.

Letting $\sigma = [\sigma_{M+1}^\top, \ldots, \sigma_{M+N}^\top]^\top$ and $\bar{\varsigma} = [\bar{\varsigma}_{M+1}^\top, \ldots, \bar{\varsigma}_{M+N}^\top]^\top$ with $\bar{\varsigma}_i = \vartheta_1\varsigma_i + \vartheta_2\mathrm{sign}^{\beta_1}(\varsigma_i) + \vartheta_3\mathrm{sign}^{\beta_2}(\varsigma_i)$, it follows from (26b) that

$$\dot{\sigma} = (\mathrm{I}_N \otimes A_0)\,\sigma - (\mathrm{I}_N \otimes \mathrm{I}_{n_0})\,\bar{\varsigma}. \tag{27}$$

Let $\varsigma_f = [\varsigma_{\bar{N}_1}^\top, \ldots, \varsigma_{\bar{N}_N}^\top]^\top$

Letting $\tilde{\sigma} = [\tilde{\sigma}_{M+1}^\top, \ldots, \tilde{\sigma}_{M+N}^\top]^\top$ and $\varsigma = [\varsigma_{M+1}^\top, \ldots, \varsigma_{M+N}^\top]^\top$, one can obtain from Lemma 1 that $\varsigma = (\mathcal{L}_F \otimes \mathrm{I}_{n_0})\sigma + (\mathcal{L}_{FF} \otimes \mathrm{I}_{n_0})\eta = (\mathcal{L}_F \otimes \mathrm{I}_{n_0})\tilde{\sigma} + (\mathcal{L}_{FF} \otimes \mathrm{I}_{n_0})\tilde{\eta}$. Then, via (9b) and (27), one has

$$\dot{\varsigma} = (\mathrm{I}_N \otimes A_0)\,\varsigma - (\mathcal{L}_F \otimes \mathrm{I}_{n_0})\,\bar{\varsigma} - (\mathcal{L}_{FF} \otimes \mathrm{I}_{n_0})\bar{\theta}. \tag{28}$$

Choose the following Lyapunov function candidate,

$$V_2 = \sum_{i=1}^{N} \left(\frac{\vartheta_2 g_{f_i}}{1+\beta_1} \|\varsigma_i\|_{1+\beta_1}^{1+\beta_1} + \frac{\vartheta_3 g_{f_i}}{1+\beta_2} \|\varsigma_i\|_{1+\beta_2}^{1+\beta_2} \right) + \frac{\vartheta_1}{2}\varsigma^\top (G_F \otimes \mathrm{I}_{n_0})\varsigma. \tag{29}$$

The time derivative of (29) along (28) satisfies

$$\dot{V}_2 = \bar{\varsigma}^\top (G_F \otimes A_0)\varsigma - \frac{1}{2}\bar{\varsigma}^\top (\Delta_F \otimes \mathrm{I}_{n_0})\,\bar{\varsigma} - \bar{\varsigma}^\top (G_F \mathcal{L}_{FF} \otimes \mathrm{I}_{n_0})\bar{\theta}, \tag{30}$$

where $\Delta_F = G_F\mathcal{L}_F + \mathcal{L}_F^\top G_F \geq 2\mathrm{I}_N$. Via Young's inequality, one has $\bar{\varsigma}^\top (G_F \otimes A_0)\varsigma \leq \frac{\|G_F \otimes A_0\|^2}{2}\|\varsigma\|^2 + \frac{1}{2}\|\bar{\varsigma}\|^2$ and $-\bar{\varsigma}^\top (G_F\mathcal{L}_{FF} \otimes \mathrm{I}_{n_0})\bar{\theta} \leq \frac{1}{2}\|\bar{\varsigma}\|^2 + \Delta_{\bar{\theta}}$, where $\Delta_{\bar{\theta}} = \frac{1}{2}\|(G_F\mathcal{L}_{FF} \otimes \mathrm{I}_{n_0})\bar{\theta}\|^2$. Thus, $\dot{V}_2$ can be further bounded by

$$\dot{V}_2 \leq \frac{\|G_F \otimes A_0\|^2}{2}\|\varsigma\|^2 + \Delta_{\bar{\theta}} \leq k_\theta V_2 + \Delta_{\bar{\theta}}, \tag{31}$$

where $k_\theta = \frac{\|G_F \otimes A_0\|^2}{\vartheta_1 g_{f\min}}$ and $g_{f\min} = \min\{g_{f_1}, \ldots, g_{f_N}\}$.

Via Lemma 3, one has η and consequently $\Delta_{\bar{\theta}}$ are bounded in $t \in [0, T_\eta)$. It then follows from (31) that $V_2(t)$ is also bounded on the same interval, which means that ς is bounded as well. Noting that $\varsigma = (\mathcal{L}_F \otimes \mathrm{I}_{n_0})\sigma + (\mathcal{L}_{FF} \otimes \mathrm{I}_{n_0})\eta$ and $\mathcal{L}_F$ is nonsingular, one has σ_i is bounded in $[0, T_\eta)$.

Step 2: $\mathbf{FIX_t}$ convergence of $\tilde{\sigma}_i$.

When $t \geq T_\eta$, one can obtain that $\tilde{\eta}_i = 0$ and $\Delta_{\bar{\theta}} = 0$. Then, it can be obtained from (28) that

$$\dot{\varsigma} = (\mathrm{I}_N \otimes A_0)\,\varsigma - (\mathcal{L}_F \otimes \mathrm{I}_{n_0})\,\bar{\varsigma}. \tag{32}$$

The time derivative of V_2 described in (29) along the trajectories of (32) satisfies

$$\dot{V}_2 \leq \bar{\varsigma}^\top (G_F \otimes A_0)\varsigma - \frac{1}{2}\bar{\varsigma}^\top (\Delta_F \otimes I_{n_0})\,\bar{\varsigma}. \tag{33}$$

Noting that $\Delta_F \geq 2\mathrm{I}_N$ and $\bar{\varsigma}^\top (G_F \otimes A_0)\varsigma \leq \frac{\|G_F \otimes A_0\|^2}{2}\|\varsigma\|^2 + \frac{1}{2}\|\bar{\varsigma}\|^2$, $\dot{V}_2$ can be further bounded by

$$\dot{V}_2 \leq \frac{1}{2}(\|G_F \otimes A_0\|^2\|\varsigma\|^2 - \|\bar{\varsigma}\|^2). \tag{34}$$

Note that $\|\bar{\varsigma}\|^2 = \sum_{i=1}^N \|\bar{\varsigma}_i\|^2 \geq \sum_{i=1}^N \vartheta_1^2\|\varsigma_i\|^2 + \sum_{i=1}^N \vartheta_2^2\|\varsigma_i\|_{2\beta_1}^{2\beta_1} + \sum_{i=1}^N \vartheta_3^2\|\varsigma_i\|_{2\beta_2}^{2\beta_2}$. Since $0 < \beta_1 < 1$ and $\beta_2 > 1$, by Lemma 6, one has $\sum_{i=1}^N \|\varsigma_i\|_{2\beta_1}^{2\beta_1} \geq \left(\|\varsigma\|^2\right)^{\beta_1}$ and $\sum_{i=1}^N \|\varsigma_i\|_{2\beta_2}^{2\beta_2} \geq \frac{1}{(n_0N)^{\beta_2-1}}\left(\|\varsigma\|^2\right)^{\beta_2}$. It then follows that

$$\|\bar{\varsigma}\|^2 \geq \vartheta_1^2\|\varsigma\|^2 + \vartheta_2^2\left(\|\varsigma\|^2\right)^{\beta_1} + \frac{\vartheta_3^2\left(\|\varsigma\|^2\right)^{\beta_2}}{(n_0N)^{\beta_2-1}}. \tag{35}$$

Substituting (35) into (34), one has

$$\dot{V}_2 \leq -c_\varsigma \left(\|\varsigma\|^2 + \left(\|\varsigma\|^2\right)^{\beta_1} + \left(\|\varsigma\|^2\right)^{\beta_2}\right), \tag{36}$$

where $c_\varsigma = \min\{\frac{\vartheta_1^2 - \|G_F \otimes A_0\|^2}{2}, \frac{\vartheta_2^2}{2}, \frac{\vartheta_3^2}{2(n_0 N)^{\beta_2 - 1}}\} > 0$.

Since $0 < \beta_1 < 1$ and $\beta_2 > 1$, via Lemma 6, one has $\sum_{i=1}^N \frac{\vartheta_2 g_{f_i}}{1+\beta_1}\|\varsigma_i\|_{1+\beta_1}^{1+\beta_1} \leq \bar{\vartheta}_2(\|\varsigma\|^2)^{\frac{1+\beta_1}{2}}$ and $\sum_{i=1}^N \frac{\vartheta_3 g_{f_i}}{1+\beta_2}\|\varsigma_i\|_{1+\beta_2}^{1+\beta_2} \leq \bar{\vartheta}_3(\|\varsigma\|^2)^{\frac{1+\beta_2}{2}}$, where $\bar{\vartheta}_2 = (\frac{\vartheta_2 g_{f\max}}{1+\beta_1})(n_0 N)^{\frac{1-\beta_1}{2}}$, $\bar{\vartheta}_3 = \frac{\vartheta_3 g_{f\max}}{1+\beta_2}$, and $g_{f\max} = \max\{g_{f_1}, \ldots, g_{f_N}\}$. Noting that $0 < \frac{2\beta_1}{1+\beta_1} < 1$ and $\frac{2\beta_2}{1+\beta_2} > 1$, via Lemma 6 and (29), one then has

$$V_2^{\frac{2\beta_1}{1+\beta_1}} \leq c_{\beta_1}\left((\|\varsigma\|^2)^{\frac{2\beta_1}{1+\beta_1}} + (\|\varsigma\|^2)^{\beta_1} + (\|\varsigma\|^2)^{\frac{\beta_1(1+\beta_2)}{1+\beta_1}}\right), \tag{37}$$

and

$$V_2^{\frac{2\beta_2}{1+\beta_2}} \leq c_{\beta_2}\left((\|\varsigma\|^2)^{\frac{2\beta_2}{1+\beta_2}} + (\|\varsigma\|^2)^{\frac{\beta_2(1+\beta_1)}{1+\beta_2}} + (\|\varsigma\|^2)^{\beta_2}\right), \tag{38}$$

where $c_{\beta_1} = \max\{(\frac{\vartheta_1 g_{f,\max}}{2})^{\frac{2\beta_1}{1+\beta_1}}, \bar{\vartheta}_2^{\frac{2\beta_1}{1+\beta_1}}, \bar{\vartheta}_3^{\frac{2\beta_1}{1+\beta_1}}\}$ and $c_{\beta_2} = \max\{(\frac{\vartheta_1 g_{f,\max}}{2})^{\frac{2\beta_2}{1+\beta_2}}, \bar{\vartheta}_2^{\frac{2\beta_2}{1+\beta_2}}, \bar{\vartheta}_3^{\frac{2\beta_2}{1+\beta_2}}\} \times 3^{\frac{\beta_2-1}{\beta_2+1}}$. Noting that $\beta_1 < \frac{2\beta_1}{1+\beta_1} < 1$ and $\beta_1 < \frac{\beta_1(1+\beta_2)}{1+\beta_1} < \beta_2$, one has $(\|\varsigma\|^2)^{\frac{2\beta_1}{1+\beta_1}} \leq \|\varsigma\|^2 + (\|\varsigma\|^2)^{\beta_1}$ and $(\|\varsigma\|^2)^{\frac{\beta_1(1+\beta_2)}{1+\beta_1}} \leq (\|\varsigma\|^2)^{\beta_1} + (\|\varsigma\|^2)^{\beta_2}$. Since $1 < \frac{2\beta_2}{1+\beta_2} < \beta_2$ and $\beta_1 < \frac{\beta_2(1+\beta_1)}{1+\beta_2} < \beta_2$, one has $(\|\varsigma\|^2)^{\frac{\beta_1(1+\beta_2)}{1+\beta_1}} \leq (\|\varsigma\|^2)^{\beta_1} + (\|\varsigma\|^2)^{\beta_2}$ and $(\|\varsigma\|^2)^{\frac{\beta_2(1+\beta_1)}{1+\beta_2}} \leq (\|\varsigma\|^2)^{\beta_1} + (\|\varsigma\|^2)^{\beta_2}$. It then follows from (37) and (38) that

$$V_2^{\frac{2\beta_1}{1+\beta_1}} \leq c_{\beta_1}\left(\|\varsigma\|^2 + 3(\|\varsigma\|^2)^{\beta_1} + (\|\varsigma\|^2)^{\beta_2}\right), \tag{39}$$

and

$$V_2^{\frac{2\beta_2}{1+\beta_2}} \leq c_{\beta_2}\left(\|\varsigma\|^2 + 3(\|\varsigma\|^2)^{\beta_2} + (\|\varsigma\|^2)^{\beta_1}\right). \tag{40}$$

Combining (39) and (40), one has

$$\frac{V_2^{\frac{2\beta_1}{1+\beta_1}}}{4c_{\beta_1}} + \frac{V_2^{\frac{2\beta_2}{1+\beta_2}}}{4c_{\beta_2}} \leq \left(\|\varsigma\|^2 + (\|\varsigma\|^2)^{\beta_1} + (\|\varsigma\|^2)^{\beta_2}\right). \tag{41}$$

Substituting (41) into (36), one has

$$\dot{V}_2 \leq -\frac{c_\varsigma}{4c_{\beta_1}}V_2^{\frac{2\beta_1}{1+\beta_1}} - \frac{c_\varsigma}{4c_{\beta_2}}V_2^{\frac{2\beta_2}{1+\beta_2}}. \tag{42}$$

According to Lemma 7 and (42), system (32) is $\mathbf{FIX_t}$ stable. The associated settling time satisfies $T_\sigma \leq \frac{4c_{\beta_1}(1+\beta_1)}{c_\varsigma(1-\beta_1)} + \frac{4c_{\beta_2}(1+\beta_2)}{c_\varsigma(\beta_2-1)} + T_\eta$. Moreover, when $t \geq T_\eta$, one has $\varsigma(t) = (\mathcal{L}_F \otimes \mathrm{I}_{n_0})\tilde{\sigma}(t)$. Since $\mathcal{L}_F$ is nonsingular, we have $\lim_{t\to T_\sigma}\tilde{\sigma}_i(t) = 0$ and $\tilde{\sigma}_i(t) = 0$ for $t \geq T_\sigma$. The lemma is thus proved. □

Lemma 5. *Consider the distributed observers (26c) under Assumptions 1 and 2. Let $\imath_1$, $\imath_2$, $\imath_3$, γ_1, and γ_2, be chosen such that $\imath_1 > \|G_F \otimes A_h\|$, $\imath_2 > 0$, $\imath_3 > 0$, $0 < \gamma_1 < 1$, $\gamma_2 > \frac{1}{\gamma_1} > 1$. There is a settling time $T_\phi \geq 0$, independent of the initial conditions, such that*

$$\lim_{t\to T_\phi}\left(\phi_i(t) - \mathrm{Co}\left(h_{xj}(t), j \in \mathcal{O}_{fl}\right)\right) = 0,$$

$$\phi_i(t) - \mathrm{Co}\left(h_{xj}(t), j \in \mathcal{O}_{fl}\right) = 0,\ t \geq T_\phi,\ \forall i \in \mathcal{O}_f. \tag{43}$$

Proof. Let $\phi = [\phi_{M+1}^\top, \ldots, \phi_{M+N}^\top]^\top$ and $\bar{\varphi} = [\bar{\varphi}_{M+1}^\top, \ldots, \bar{\varphi}_{M+N}^\top]^\top$ with $\bar{\varphi}_i = \imath_1\varphi_i + \imath_2\mathrm{sign}^{\gamma_1}(\varphi_i) + \imath_3\mathrm{sign}^{\gamma_2}(\varphi_i)$. It follows from (26c) that

$$\dot{\phi} = (\mathrm{I}_N \otimes A_h)\,\phi - (\mathrm{I}_N \otimes \mathrm{I}_l)\,\bar{\varphi}. \tag{44}$$

Defining $\tilde{\phi} = \phi - \left((-\mathcal{L}_F^{-1}\mathcal{L}_{FF}) \otimes \mathrm{I}_l\right)h_{FF}$ and $h_{FF} = [h_{x1}^\top, \ldots, h_{xM}]^\top$, it follows from (4) and (44) that

$$\dot{\tilde{\phi}} = (\mathrm{I}_N \otimes A_h)\,\tilde{\phi} - (\mathrm{I}_N \otimes \mathrm{I}_l)\,\bar{\varphi}. \tag{45}$$

Let $\varphi = [\varphi_{M+1}^\top, \ldots, \varphi_{M+N}^\top]^\top$. One can obtain from Lemma 1 that $\varphi = (\mathcal{L}_F \otimes \mathrm{I}_l)\tilde{\phi}$. Then, via (45), one has

$$\dot{\varphi} = (\mathrm{I}_N \otimes A_h)\,\varphi - (\mathcal{L}_F \otimes \mathrm{I}_l)\,\bar{\varphi}. \tag{46}$$

It is noted that equation (46) has the same structure as equation (32). Using the same procedure as in the proof of the $\mathbf{FIX_t}$ convergence of $\varsigma(t)$, it follows that there is a settling time $T_\phi \geq 0$, independent of the initial conditions, such that $\lim_{t\to T_\phi}\varphi_i(t) = 0$ and $\varphi_i(t) = 0$ for $t \geq T_\phi$. Note that $\mathcal{L}_F$ is nonsingular and $-\mathcal{L}_F^{-1}\mathcal{L}_{FF}$ has the following form

$$-\mathcal{L}_F^{-1}\mathcal{L}_{FF} \triangleq \begin{pmatrix} \rho_{\bar{M}_1 1} & \cdots & \rho_{\bar{M}_1 M} \\ \vdots & \ddots & \vdots \\ \rho_{\bar{M}_N 1} & \cdots & \rho_{\bar{M}_N M} \end{pmatrix}.$$

Then, one has $\lim_{t\to T_\phi}(\phi_i - \sum_{j=1}^M \rho_{ij}h_{xj}) = 0$ and $\phi_i - \sum_{j=1}^M \rho_{ij}h_{xj} = 0$ for $t \geq T_\phi$, where $\sum_{j=1}^M \rho_{ij} = 1$ and $\rho_{ij} \geq 0$, that is, $\lim_{t\to T_\phi}\left(\phi_i - \mathrm{Co}\left(h_{xj}, j \in \mathcal{O}_{fl}\right)\right) = 0$ and $\phi_i - \mathrm{Co}\left(h_{xj}, j \in \mathcal{O}_{fl}\right) = 0$ for $t \geq T_\phi$. The proof is thus completed. □

Now, we proceed to design the $\mathbf{FIX_t}$ containment control component v_i in (26a). Define $\hat{e}_{c,i} = x_i - \Xi_i\sigma_i - \Xi_{hi}\phi_i$, $i \in \mathcal{O}_f$. Since $\mathrm{rank}(B_i) = m_i$, via Lemmas 1 and 8, there is a linear coordinate transformation $\hat{\ell}_i = T_i\hat{e}_{c,i} = [\hat{\ell}_{i1,1}, \ldots, \hat{\ell}_{i1,\rho_1}, \ldots, \hat{\ell}_{im_i,1}, \ldots, \hat{\ell}_{im_i,\rho_{m_i}}]^\top$, where ρ_j, $j = 1, \ldots, m_i$, denotes the controllability index of $\hat{\ell}_{ij}$. Then, v_i is proposed as follows:

$$v_i = M_i^{-1}(\omega_i - D_i\hat{e}_{c,i}), \tag{47}$$

where $\omega_i = [\omega_{i1}, \ldots, \omega_{ij}, \ldots, \omega_{im_i}]^\top$ with $\omega_{ij} = -\sum_{k=1}^{\rho_j}\left(c_{ij,k}\mathrm{sign}^{p_{ij,k}}(\hat{\ell}_{ij,k}) + \bar{c}_{ij,k}\mathrm{sign}^{\bar{p}_{ij,k}}(\hat{\ell}_{ij,k})\right)$, D_i and invertible matrix M_i are designed as in Lemma 8, $c_{ij,k}$, $\bar{c}_{ij,k}$, $p_{ij,k}$, and $\bar{p}_{ij,k}$, $j = 1, \ldots, m_i$, $k = 1, \ldots, \rho_j$, $i \in \mathcal{O}_f$, can be given as in Lemma 9.

The main result of this subsection is presented below.

Theorem 2. *Suppose Assumptions 1-5 hold. Consider the MAS described in (1) and (2). The FXFCT problem described in Definition 1 is solved under the $\mathbf{FIX_t}$ distributed formation tracking control protocols (9) and (23) for the formation-leaders and the $\mathbf{FIX_t}$ distributed containment control protocols (26) and (47) for the followers.*

Proof. Similar to the proof of Theorem 1, this theorem is proved in two steps. Firstly, the containment errors are proved to be bounded in $[0, T_m)$, where $T_m = \max\{T_\sigma, T_\phi\}$. Then,

This article has been accepted for publication in IEEE Transactions on Automation Science and Engineering. This is the author's version which has not been fully edited and content may change prior to final publication. Citation information: DOI 10.1109/TASE.2026.3713131

we show that not only formation tracking errors but also containment errors converge to zero in a fixed time.

Step 1: Under Assumptions 4 and 5, one can obtain from (1), (26b), and (26c) that

$$\dot{\hat{e}}_{c,i} = A_i \hat{e}_{c,i} + B_i v_i + \Xi_i \bar{\varsigma}_i + \Xi_{hi} \bar{\varphi}_i. \tag{48}$$

Let $\hat{\ell}_i = T_i \hat{e}_{c,i} = [\hat{\ell}_{i1,1}, \ldots, \hat{\ell}_{i1,\rho_1}, \ldots, \hat{\ell}_{im_i,1}, \ldots, \hat{\ell}_{im_i,\rho_{m_i}}]^\top$ and $\Delta_{ci} = T_i(\Xi_i \bar{\varsigma}_i + \Xi_{hi} \bar{\varphi}_i) = [\Delta_{ci1,1}, \ldots, \Delta_{ci1,\rho_1}, \ldots, \Delta_{cim_i,1}, \ldots, \Delta_{cim_i,\rho_{m_i}}]^\top$. Then, the dynamics of $\hat{\ell}_{ij}$, $j = 1, \ldots, m_i$, have the following form,

$$\begin{cases} \dot{\hat{\ell}}_{ij,1} = \hat{\ell}_{ij,2} + \Delta_{cij,1}, \\ \dot{\hat{\ell}}_{ij,2} = \hat{\ell}_{ij,3} + \Delta_{cij,2}, \\ \quad \vdots \\ \dot{\hat{\ell}}_{ij,\rho_j} = \omega_{ij} + \Delta_{cij,\rho_j}, \end{cases} \tag{49}$$

where $\omega_{ij} = -\sum_{k=1}^{\rho_j} \left(c_{ij,k} \mathrm{sign}^{p_{ij,k}}(\hat{\ell}_{ij,k}) + \bar{c}_{ij,k} \mathrm{sign}^{\bar{p}_{ij,k}}(\hat{\ell}_{ij,k}) \right)$. Similar to the analysis of the boundedness of $\hat{\zeta}$ in Theorem 1, it follows that system (49) is BIBS stable, provided that $\Delta_{cij} = [\Delta_{cij,1}, \ldots, \Delta_{cij,\rho_j}]^\top$ is considered as an input. Via Lemmas 4 and 5, one has $\Xi_i \bar{\varsigma}_i + \Xi_{hi} \bar{\varphi}_i$ is bounded, and consequently Δ_{cij}, $j = 1, \ldots, m_i$, are bounded in $[0, T_m)$. As a result, $\hat{\ell}_i$ is bounded in $[0, T_m)$. Since $\hat{\ell}_i = T_i \hat{e}_{c,i}$ and T_i is nonsingular, it follows that $\hat{e}_{c,i}$ is bounded in $[0, T_m)$.

Step 2: From Lemmas 4 and 5, one has that $\sigma_i = x_0$ and $\phi_i = \mathrm{Co}\,(h_{xj}, j \in \mathcal{O}_{fl})$ hold for $t \geq T_m$, which implies that $\hat{e}_{c,i} = e_{c,i} = x_i - \Xi_i x_0 - \Xi_{hi} \mathrm{Co}\,(h_{xj}, j \in \mathcal{O}_{fl})$ and $\Delta_{ci} = 0$.

Via Lemma 9, it follows that system (49) is $\mathbf{FIX_t}$ stable for all $j \in \{1, \ldots, m_i\}$. The settling time satisfies $T_c \leq T_m + T_\ell$, where T_ℓ can be determined based on Lemma 9.

Noting that $\ell_i(t) = T_i e_{c,i}(t)$ and T_i is invertible, one has $\lim_{t \to T_c} e_{c,i}(t) = 0$ and $e_{c,i}(t) = 0$ for $t \geq T_c$. Via Lemma 1 and Theorem 1, one has $e_{Fi}(t) = C_i e_{c,i}(t) - \mathrm{Co}(e_{Lj}(t), j \in \mathcal{O}_{fl}) = y_i(t) - \mathrm{Co}\,(y_j(t), j \in \mathcal{O}_{fl}) - \mathrm{Co}(e_{Lj}(t), j \in \mathcal{O}_{fl})$. It follows from Theorem 1 that $\lim_{t \to T_{fl}} e_{Lj}(t) = 0$ and $e_{Lj}(t) = 0$ for $t \geq T_{fl}$. Then, it can be obtained that $\lim_{t \to T} e_{Fi}(t) = 0$ and $e_{Fi}(t) = 0$ for $t \geq T$, where $T = \max\{T_c, T_{fl}\}$. Thus, equation (6) is achieved. Combining the results in Theorem 1, the FXFCT control problem described by Definition 1 is solved. □

Remark 3. *The invertibility of M_i in* (23) *and* (47) *is guaranteed by Lemma 8. Specifically, under Assumption 3 and the condition* $\mathrm{rank}(B_i) = m_i$, *the controllability-index-based coordinate transformation yields an invertible matrix M_i in the transformed error dynamics. This property provides the basis for designing z_i and v_i for the formation-leaders and followers, respectively.*

Remark 4. *Through a linear coordinate transformation, systems* (24) *and* (48) *are transformed into m_i single-input subsystems in controllable canonical form. For each subsystem, the coupling terms involving the transformed error variables appear only in the last equation of the corresponding integrator chain. Based on this structure, the $\mathbf{FIX_t}$ control schemes can be designed without requiring the construction of a matrix K_{i4} satisfying $B_i K_{i4} = \mathrm{I}_{n_i}$. Therefore, the proposed design relaxes the full-row-rank condition imposed in [51], thereby broadening the applicability of the proposed method to a wider class of MASs.*

Remark 5. *In practical implementation, discrete sampling, model uncertainties, external disturbances, and other nonideal effects may prevent tracking errors from converging exactly to zero. However, for engineering applications, it is often sufficient to ensure that tracking errors become sufficiently small within a fixed time. From this perspective, the proposed continuous-time fixed-time control law can still be effective in a discrete implementation.*

IV. Simulation Examples

A. Example 1

In this example, the HMAS is composed of one reference leader, four formation-leaders, and four followers. The interaction topology is illustrated in Figure 2.

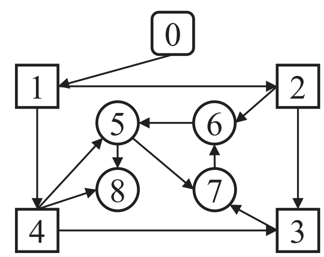

Figure 2. Interaction topology.

The system matrices for the formation-leaders and followers are borrowed from [55] and are described as follows,

$$A_i = \begin{pmatrix} 0 & 1 & 0 \\ 0 & d_i & c_i \\ 0 & b_i & a_i \end{pmatrix},\ B_i = \begin{pmatrix} 0 & 0 \\ e_i & 0 \\ 0 & f_i \end{pmatrix},$$
$$C_i = \begin{pmatrix} 1 & 0 & 0 \\ 0 & 1 & 0 \end{pmatrix},\ i = 1, \cdots, 8,$$

where the parameters $\{a_i, b_i, c_i, d_i, e_i, f_i\}$ are chosen as $\{-1, -1, 2, 1, 1, 1\}$, $\{-2, -1, 1, 0, 1, 1\}$, $\{-2, 0, 2, 1, 1, 1\}$, $\{-3, -1, 1, 0, 1, 1\}$, $\{-4, -1, 1, 1, 1, 1\}$, $\{-8, -1, 2, 0, 1, 1\}$, $\{-2, -2, 1, 1, 1, 1\}$, and $\{-3, 0, 2, 0, 1, 1\}$.

The system matrices of the reference leader (2) are described by,

$$A_0 = \begin{pmatrix} 0 & 1 & 0 \\ -1 & 0 & 0 \\ 0 & 0 & 0 \end{pmatrix}, C_0 = \begin{pmatrix} 1 & 0 & 0 \\ 0 & 1 & 0 \end{pmatrix}.$$

The TVF vector is set as follows,

$$h_{xi} = 4 \begin{pmatrix} -\cos\left(t + \frac{(i-1)\pi}{2}\right) \\ \sin\left(t + \frac{(i-1)\pi}{2}\right) \end{pmatrix},\ i = 1, 2, 3, 4,$$

and $h_{yi} = h_{xi}$. Solving the equations (7)-(8) yields

$$\Xi_i = \begin{pmatrix} 1 & 0 & 0 \\ 0 & 1 & 0 \\ e_i & 0 & 1 \end{pmatrix},\ \Gamma_i = \begin{pmatrix} \frac{-1-c_i e_i}{e_i} & -\frac{d_i}{e_i} & -\frac{c_i}{e_i} \\ -\frac{a_i e_i}{f_i} & \frac{-b_i}{f_i} & \frac{-a_i}{f_i} \end{pmatrix},$$

This article has been accepted for publication in IEEE Transactions on Automation Science and Engineering. This is the author's version which has not been fully edited and content may change prior to final publication. Citation information: DOI 10.1109/TASE.2026.3713131

$$\Xi_{hi} = \begin{pmatrix} 1 & 0 \\ 0 & 1 \\ 0 & e_i \end{pmatrix}, \Gamma_{hi} = \begin{pmatrix} \frac{-1}{e_i} & \frac{-d_i - c_i e_i}{e_i} \\ \frac{-e_i}{f_i} & \frac{-b_i - a_i e_i}{f_i} \end{pmatrix}.$$

The parameters in the $\mathbf{FIX_t}$ formation tracking controller (9) and containment controller (26) are chosen as $\mu_1 = 7$, $\vartheta_1 = \imath_1 = 3$, $\mu_2 = \vartheta_2 = \imath_2 = 5$, $\mu_3 = \vartheta_3 = \imath_3 = 6$, $\alpha_1 = \beta_1 = \gamma_1 = 7/9$, $\alpha_2 = \beta_2 = \gamma_2 = 907/700$, and $M_i = \mathrm{I}_2$, $i = 1, \ldots, 8$. The initial states of the HMAS are randomly set within the interval $[-4, 4]$. The initial conditions for the distributed observers are chosen as zeros.

The simulation results are presented in Figures 3-5. The snapshots of the HMAS at $t = 0$s and $t = 10$s are illustrated in Figure 3. The outputs of the reference leader, formation-leaders, and followers are marked by a pentagram, square markers, and circle markers, respectively. The gray plane formed by connecting the square markers corresponds to the convex hull spanned by the formation-leaders. As observed from Figure 3, the formation-leaders not only form a quadrilateral TVF and track the trajectory provided by the reference leader in a fixed time, but also the outputs of the followers converge to the convex hull spanned by those of the formation-leaders. The estimation errors of the distributed $\mathbf{FIX_t}$ observers are shown in Figure 4. The formation tracking errors and the output containment errors are given in Figures 5(a) and 5(b), respectively.

For comparison, Figure 6 shows the FCT errors obtained using a $\mathbf{FIN_t}$ controller, which is derived by modifying the proposed control scheme to exclude the power terms with exponents greater than one. The same initial conditions are adopted for both cases. The comparison between Figures 5 and 6 demonstrates that the performance of the $\mathbf{FIX_t}$ controller is much better than its $\mathbf{FIN_t}$ counterpart.

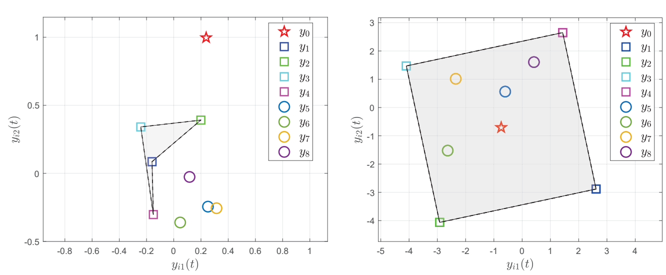

(a) (b)

Figure 3. The output snapshots of the MAS. (a) $t = 0$s. (b) $t = 10$s.

B. Example 2

This example demonstrates the proposed FXFCT control method in an air–ground cooperative scenario involving a heterogeneous multi-robot system, as illustrated in Figure 7. The system consists of four quadrotor AAVs as formation-leaders ($\mathcal{O}_{fl} = \{1, 2, 3, 4\}$) and four AGVs as followers ($\mathcal{O}_f = \{5, 6, 7, 8\}$). Additionally, a reference leader ($i = 0$) generates the reference trajectory for the entire system. The communication topology is identical to that in *Example 1*.

Since the altitude of each AAV can be controlled independently, we focus on the planar motion in the XY plane in the following analysis. Following the inner/outer loop control

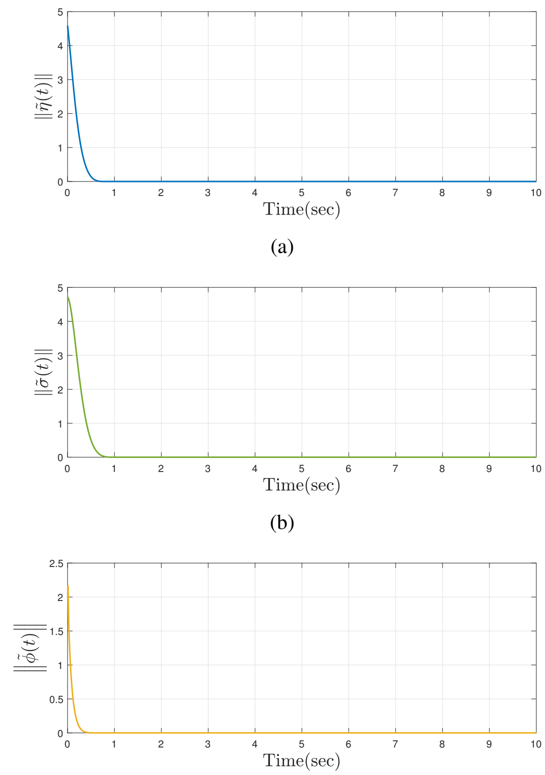

Figure 4. The estimation errors of the distributed $\mathbf{FIX_t}$ observers: (a) $\|\tilde{\eta}\|$. (b) $\|\tilde{\sigma}\|$. (c) $\|\tilde{\phi}\|$

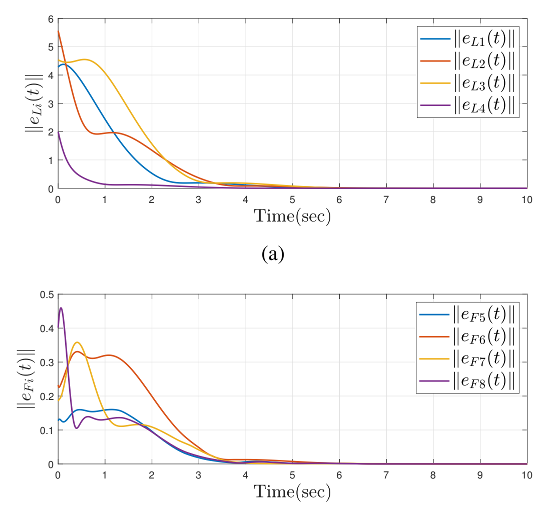

Figure 5. (a) The formation tracking errors with the $\mathbf{FIX_t}$ controller. (b) The containment errors with the $\mathbf{FIX_t}$ controller.

architecture in [56], the outer-loop dynamics of the four AAVs are modeled as,

$$\begin{cases} \dot{x}_j = v_j, \\ \dot{v}_j = c_{x_j} x_j + c_{v_j} v_j + u_j, \ j \in \mathcal{O}_{fl}, \end{cases}$$

where x_j, v_j, and u_j denote the position, velocity, and control input, respectively, and c_{x_j} and c_{v_j} are constant

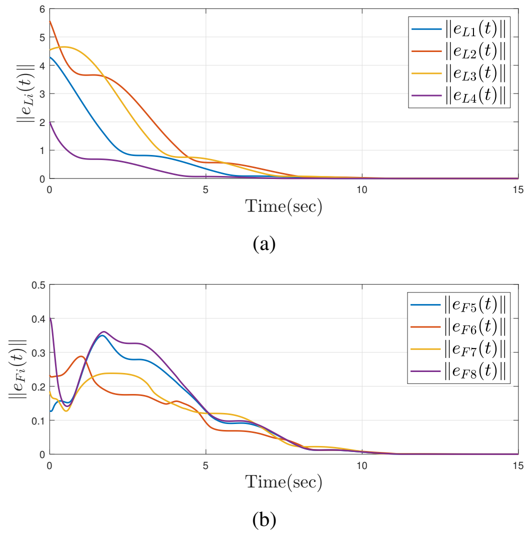

Figure 6. (a) The formation tracking errors with the $\mathbf{FIN_t}$ controller. (b) The containment errors with the $\mathbf{FIN_t}$ controller.

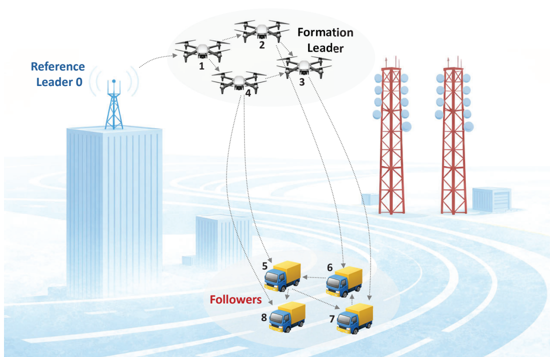

Figure 7. Heterogeneous multi-robot system.

feedback coefficients. The coefficients are set to $\{c_{x_1}, c_{v_1}\} = \{-1, -1\}$, $\{c_{x_2}, c_{v_2}\} = \{-2, -2\}$, $\{c_{x_3}, c_{v_3}\} = \{-3, -3\}$, and $\{c_{x_4}, c_{v_4}\} = \{0, 0\}$.

Following [20], the dynamics of the four AGVs are given by

$$\dot{x}_k = u_k, \ k \in \mathcal{O}_f,$$

where x_k and u_k denote the position and control input, respectively.

The system matrices of the reference leader are $A_0 = \mathrm{I}_2 \otimes \begin{pmatrix} 0 & 1 \\ -1 & 0 \end{pmatrix}$ and $C_0 = \mathrm{I}_2 \otimes \begin{pmatrix} 1 & 0 \end{pmatrix}$. All AAVs move in the horizontal plane at a constant altitude $z = 3$ m. For $j \in \mathcal{O}_{fl}$, the TVF vectors are

$$h_{xj}(t) = \begin{pmatrix} 4\cos\left(t + (j-1)\pi/2\right) \\ -4\sin\left(t + (j-1)\pi/2\right) \\ 4\sin\left(t + (j-1)\pi/2\right) \\ 4\cos\left(t + (j-1)\pi/2\right) \end{pmatrix},$$

and $h_{yj}(t) = \begin{pmatrix} 4\cos(t + (j-1)\pi/2) \\ 4\sin\left(t + (j-1)\pi/2\right) \end{pmatrix}$. Solving the regulator equations (7)–(8) yields $\Xi_j = \Xi_{hj} = \mathrm{I}_4$, $\Xi_k = \Xi_{hk} = \mathrm{I}_2 \otimes \begin{pmatrix} 1 & 0 \end{pmatrix}$, $\Gamma_j = \Gamma_{hj} = \mathrm{I}_2 \otimes \begin{pmatrix} -1 - c_{x_j} & -c_{v_j} \end{pmatrix}$, and $\Gamma_k = \Gamma_{hk} = \mathrm{I}_2 \otimes \begin{pmatrix} 0 & 1 \end{pmatrix}$, where $j \in \mathcal{O}_{fl}$ and $k \in \mathcal{O}_f$. Let $x_0(0) = (10 \ -2 \ 2 \ 10)^\top$, and set the remaining initial conditions (AAVs, AGVs, and distributed observers) as in *Example 1*.

Figures 8 and 9 illustrate the simulation results. Figure 8 shows the output trajectories of the heterogeneous multi-robot system. The four AAVs, operating at an altitude of $z = 3$ m, form a rotating quadrilateral TVF while tracking the reference trajectory, which is marked by the red pentagram. Meanwhile, the four AGVs on the ground plane converge into the projection of the convex hull spanned by the AAVs. Figure 9 presents the FXFCT error. These results demonstrate the effectiveness of the proposed control method in the air–ground cooperative scenario.

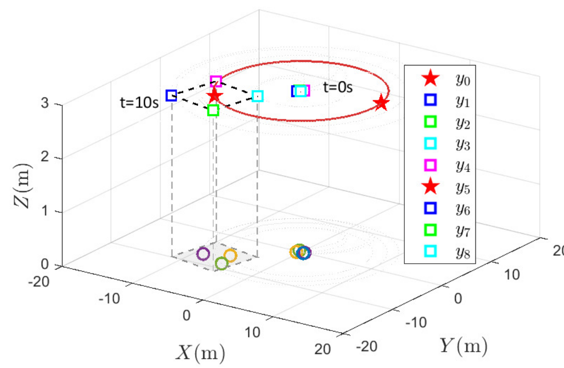

Figure 8. The output trajectories of the heterogeneous multi-robot system.

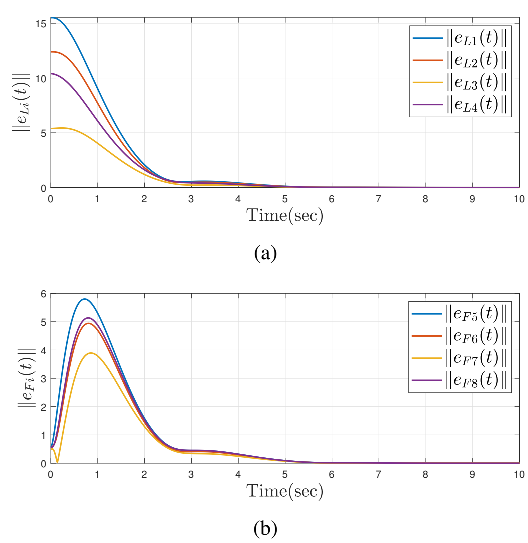

Figure 9. (a) The formation tracking errors. (b) The containment errors.

V. Conclusion

This paper has studied the FXFCT control problem of HMASs under the directed graph. Novel distributed $\mathbf{FIX_t}$

control protocols have been developed for both the formation-leaders and followers. Under these proposed control protocols, the outputs of the formation-leaders achieve a desired TVF and simultaneously track the trajectory provided by the reference leader in a fixed time. Meanwhile, the output of followers can converge to the convex hull spanned by the outputs of the formation-leaders in a fixed time. Moreover, results on $\mathbf{FIN_t}$ or $\mathbf{FIX_t}$ consensus tracking, formation tracking, and containment control of linear MASs are encompassed as special instances of the proposed approach. Future work will investigate the sampled-data FXFCT problem for HMASs.

Appendix

Lemma 6 ([57]). *For any $\chi_i \in \mathbb{R}$, $i = 1, 2, \ldots, n$, and any $p \in (0, 1]$, $\left(\sum_{i=1}^{n} |\chi_i|\right)^p \le \sum_{i=1}^{n} |\chi_i|^p \le n^{1-p} \left(\sum_{i=1}^{n} |\chi_i|\right)^p$. For any $p > 1$, $\sum_{i=1}^{n} |\chi_i|^p \le \left(\sum_{i=1}^{n} |\chi_i|\right)^p \le n^{p-1} \sum_{i=1}^{n} |\chi_i|^p$.*

Lemma 7 ([44]). *Consider the system with dynamics described by $\dot{x} = g(x, t)$, where $g : \mathbb{R}^n \times [0, \infty) \to \mathbb{R}^n$ is a nonlinear function, which can be discontinuous. Assume that a continuous, positive-definite, and radially unbounded function function $W(x) : \mathbb{R}^n \to \mathbb{R}$ exists such that $\dot{W}(x) \le -a_1(W(x))^p - a_2(W(x))^q$ for all $x \in \mathbb{R}^n$, where $a_1 > 0$, $a_2 > 0$, $0 < p < 1$, and $q > 1$. Then, the system is $\mathbf{FIX_t}$ stable, and the convergence time satisfies $T \le \frac{1}{a_1(1-p)} + \frac{1}{a_2(q-1)}$.*

Lemma 8 ([58]). *For a linear system*

$$\dot{x} = Ax + Bu, \tag{50}$$

where $x \in \mathbb{R}^n$, $u \in \mathbb{R}^m$, A and B are the constant matrices.

Given that (A, B) is controllable and $\mathrm{rank}(B) = m$, one can find a nonsingular transformation matrix $T \in \mathbb{R}^{n\times n}$ such that $\xi = Tx = \left[\xi_1^\top, \ldots, \xi_m^\top\right]^\top$, where each block ξ_i corresponds to the controllability index ρ_i, $i = 1, \ldots, m$. Then, the subsystem dynamics corresponding to ξ_i, $i = 1, \ldots, m$, are given by

$$\begin{cases} \dot{\xi}_{i,1} = \xi_{i,2}, \\ \dot{\xi}_{i,2} = \xi_{i,3}, \\ \vdots \\ \dot{\xi}_{i,\rho_i} = t_i^\top A^{\rho_i}\xi + t_i^\top A^{\rho_i-1}Bu, \end{cases}$$

where $t_i^\top = i_{r_i}^\top T$, $i_k \in \mathbb{R}^n$ is the k-th canonical basis vector, and $r_i = \sum_{k=0}^{i-1}(1 + \rho_k)$ with $\rho_0 = 0$.

Moreover, define $\xi^\rho = \left[\xi_{1,\rho_1}, \ldots, \xi_{m,\rho_m}\right]^\top \in \mathbb{R}^m$, one has

$$\dot{\xi}^\rho = G\xi + Mu, \tag{51}$$

where $G = \begin{pmatrix} t_1^\top A^{\rho_1} \\ \vdots \\ t_m^\top A^{\rho_m} \end{pmatrix}$ and $M = \begin{pmatrix} t_1^\top A^{\rho_1-1}B \\ \vdots \\ t_m^\top A^{\rho_m-1}B \end{pmatrix}$ with M being invertible.

Lemma 9 ([59]). *Consider a system that is modeled as an n-th order integrator,*

$$\begin{cases} \dot{x}_1 = x_2 \\ \dot{x}_2 = x_3 \\ \vdots \\ \dot{x}_n = u \end{cases} \tag{52}$$

where $x = [x_1, \ldots, x_n]^\top$ and u denote the state and control input, respectively.

The $\mathbf{FIX_t}$ controller is established as

$$u = -\sum_{j=1}^{n} \left(\iota_j \mathrm{sign}^{\alpha_j}(x_j) + \bar{\iota}_j \mathrm{sign}^{\beta_j}(x_j)\right), \tag{53}$$

where α_j and β_j, $j = 2, \ldots, n$, can be defined recursively as $\alpha_{j-1} = \frac{\alpha_j\alpha_{j+1}}{2\alpha_{j+1}-\alpha_j}$, $\beta_{j-1} = \frac{\beta_j\beta_{j+1}}{2\beta_{j+1}-\beta_j}$, with terminal values $\alpha_{n+1} = \beta_{n+1} = 1$, $\alpha_n = \alpha \in (1-\epsilon, 1)$, and $\beta_n = \beta \in (1, 1+\bar{\epsilon})$ for sufficiently small $\epsilon, \bar{\epsilon} > 0$. The parameters $\iota_j > 0$ and $\bar{\iota}_j > 0$, $j = 1, \ldots, n$, are selected such that

$$H_1 = \begin{pmatrix} 0 & 1 & \cdots & 0 \\ \vdots & \vdots & \ddots & \vdots \\ 0 & 0 & \cdots & 1 \\ -\iota_1 & -\iota_2 & \cdots & -\iota_n \end{pmatrix}, H_2 = \begin{pmatrix} 0 & 1 & \cdots & 0 \\ \vdots & \vdots & \ddots & \vdots \\ 0 & 0 & \cdots & 1 \\ -\bar{\iota}_1 & -\bar{\iota}_2 & \cdots & -\bar{\iota}_n \end{pmatrix}.$$

are Hurwitz matrices.

The convergence time T is bounded by

$$T \le \frac{\alpha\lambda_{\max}(P_1)\lambda_{\max}^{\frac{1-\alpha}{\alpha}}(P_1)}{(1-\alpha)\lambda_{\min}(Q_1)} + \frac{\beta\lambda_{\max}(P_2)\lambda_{\max}^{\frac{\beta-1}{\beta}}(P_2)}{(\beta-1)\lambda_{\min}(Q_2)}, \tag{54}$$

where $P_i = P_i^\top > 0$ and $Q_i = Q_i^\top > 0$, $i = 1, 2$, satisfy $P_iH_i + H_i^\top P_i = -Q_i$.

References

[1] R. Olfati-Saber and R. M. Murray, “Consensus problems in networks of agents with switching topology and time-delays,” *IEEE Transactions on Automatic Control*, vol. 49, no. 9, pp. 1520–1533, 2004.

[2] Y. Mo and R. M. Murray, “Privacy preserving average consensus,” *IEEE Transactions on Automatic Control*, vol. 62, no. 2, pp. 753–765, 2016.

[3] L. Fu and L. An, “Collisions-free and connectivity-preserving distributed cooperative output regulation of nonlinear multiagent systems,” *IEEE Transactions on Automation Science and Engineering*, vol. 22, pp. 20 394–20 405, 2025.

[4] L. Zhou, S. Gao, J. Liu, C. Zhang, and Y. Li, “A distributed cooperative framework of robust trajectory tracking control for six-wheel independent driving and steering robot,” *IEEE Transactions on Automation Science and Engineering*, vol. 22, pp. 23 366–23 378, 2025.

[5] Z. Qin, T. Liu, T. Liu, Z. P. Jiang, and T. Chai, “Distributed feedback optimization of nonlinear uncertain systems subject to inequality constraints,” *IEEE Transactions on Automatic Control*, vol. 69, no. 6, pp. 3989–3996, 2024.

[6] W. Ren and R. W. Beard, “Consensus seeking in multiagent systems under dynamically changing interaction topologies,” *IEEE Transactions on Automatic Control*, vol. 50, no. 5, pp. 655–661, 2005.

[7] Y. Jiang, L. Liu, and G. Feng, “Fully distributed adaptive control for output consensus of uncertain discrete-time linear multi-agent systems,” *Automatica*, vol. 162, p. 111 531, 2024.

[8] C. Zhou, Z. Mao, X. Xie, B. Jiang, and W. Li, "Encoding–decoding-based fault-tolerant consensus control for multi-agent systems with markovian switching topologies and logarithmic quantizers," *IEEE Transactions on Automation Science and Engineering*, vol. 22, pp. 23 984–23 995, 2025.

[9] Y. H. Choi and S. J. Yoo, "Distributed quantized feedback design strategy for adaptive consensus tracking of uncertain strict-feedback nonlinear multiagent systems with state quantizers," *IEEE Transactions on Cybernetics*, vol. 52, no. 7, pp. 7069–7083, 2022.

[10] A. Anand, D. Guha, and S. Purwar, "Observer-aided adaptive consensus control of cyber-physical multi-agent systems with hybrid attacked topology," *IEEE Transactions on Automation Science and Engineering*, vol. 23, pp. 5250–5261, 2026.

[11] S. Raj, K. Shihabudheen, and J. Jacob, "Modular reservoir echo state network based adaptive consensus control of nonlinear multi-agent systems under time varying state constraints, delays and disturbances," *IEEE Transactions on Automation Science and Engineering*, 2026. DOI: 10.1109/TASE.2025.3598150

[12] R. Xi, Z. Shen, H. Huang, and H. Zhang, "Command filtered adaptive tracking consensus of random nonlinear multi-agent systems," *IEEE Transactions on Automation Science and Engineering*, vol. 22, pp. 8361–8370, 2024.

[13] B. Chen and B. Chu, "Distributed norm optimal iterative learning control for high-performance consensus tracking," *IEEE Transactions on Automatic Control*, vol. 71, no. 2, pp. 753–768, 2026.

[14] X. Guo, C. Wang, Z. Dong, and Z. Ding, "Adaptive containment control for heterogeneous MIMO nonlinear multiagent systems with unknown direction actuator faults," *IEEE Transactions on Automatic Control*, vol. 68, no. 9, pp. 5783–5790, 2022.

[15] J. Xu, P. Lin, L. Cheng, and H. Dong, "Containment control with input and velocity constraints," *Automatica*, vol. 142, p. 110 417, 2022.

[16] C. Wang, Y. Yang, L. Zou, and B. Shen, "Predictive containment control for multi-agent systems subject to denial-of-service attacks," *IEEE Transactions on Automation Science and Engineering*, vol. 22, pp. 23 177–23 189, 2025.

[17] Q. Xiong, X. Xu, X. Zhang, and X. Li, "Distributed dynamic containment problem in discrete-time switching networks," *Automatica*, vol. 183, p. 112 689, 2026.

[18] W. Yang, J. Dong, and J. Y. Park, "Observer-based containment control for multiagent systems by a node-based hybrid triggering mechanism," *IEEE Transactions on Automation Science and Engineering*, vol. 22, pp. 20 249–20 262, 2025.

[19] J. A. Fax and R. M. Murray, "Information flow and cooperative control of vehicle formations," *IEEE Transactions on Automatic Control*, vol. 49, no. 9, pp. 1465–1476, 2004.

[20] W. Ren and N. Sorensen, "Distributed coordination architecture for multi-robot formation control," *Robotics and Autonomous Systems*, vol. 56, no. 4, pp. 324–333, 2008.

[21] X. Zhang, Q. Yang, F. Xiao, H. Fang, and J. Chen, "Linear formation control of multi-agent systems," *Automatica*, vol. 171, p. 111 935, 2025.

[22] J. Zhang, J. Ning, and S. Tong, "Asynchronous resilient collision-free formation control for nonlinear MASs under DoS attacks," *Automatica*, vol. 183, p. 112 619, 2026.

[23] M. Abbasi and H. J. Marquez, "Dynamic event-triggered formation control of multi-agent systems with non-uniform time-varying communication delays," *IEEE Transactions on Automation Science and Engineering*, vol. 22, pp. 8988–9000, 2025.

[24] Y.-Y. Chen, K. Chen, and A. Astolfi, "Adaptive formation tracking control for first-order agents with a time-varying flow parameter," *IEEE Transactions on Automatic Control*, vol. 67, no. 5, pp. 2481–2488, 2021.

[25] X. Gong, J. Gui, Y. Chen, X. Yang, W. Yu, and T. Huang, "Resilient human-in-the-loop formation-tracking of multi-UAV systems against byzantine attacks," *IEEE Transactions on Automation Science and Engineering*, vol. 22, pp. 3797–3809, 2024.

[26] X. Dong and G. Hu, "Time-varying formation tracking for linear multiagent systems with multiple leaders," *IEEE Transactions on Automatic Control*, vol. 62, no. 7, pp. 3658–3664, 2017.

[27] X.-J. Peng, Y. He, Z. Liu, L. You, and H. Li, "Time-varying formation H_∞ tracking control and optimization for delayed multi-agent systems with exogenous disturbances," *IEEE Transactions on Automation Science and Engineering*, vol. 22, pp. 5637–5647, 2024.

[28] B. M. C. Silva, J. Y. Ishihara, and E. S. Tognetti, "Time-varying output formation tracking of linear disturbed multi-agent systems by dynamic protocols," *Automatica*, vol. 179, p. 112 419, 2025.

[29] B. Wang, W. Chen, B. Zhang, P. Shi, and H. Zhang, "A nonlinear observer-based approach to robust cooperative tracking for heterogeneous spacecraft attitude control and formation applications," *IEEE Transactions on Automatic Control*, vol. 68, no. 1, pp. 400–407, 2022.

[30] Z. Feng, G. Hu, X. Dong, and J. Lü, "Discrete-time adaptive distributed output observer for time-varying formation tracking of heterogeneous multi-agent systems," *Automatica*, vol. 160, p. 111 400, 2024.

[31] Z. Shi, Q. Wang, X. Lu, X. Dong, J. Lu, and D. Wang, "Robust output formation tracking for heterogeneous multiagent systems with multiple leaders: Theory and application," *IEEE Transactions on Industrial Electronics*, vol. 73, no. 1, pp. 1258–1268, 2026.

[32] X. Zhang, J. Wu, X. Zhan, T. Han, and H. Yan, "Observer-based adaptive time-varying formation-containment tracking for multiagent system with bounded unknown input," *IEEE Transactions on Systems, Man, and Cybernetics: Systems*, vol. 53, no. 3, pp. 1479–1491, 2022.

[33] J. Hu, P. Bhowmick, I. Jang, F. Arvin, and A. Lanzon, "A decentralized cluster formation containment frame-

work for multirobot systems," *IEEE Transactions on Robotics*, vol. 37, no. 6, pp. 1936–1955, 2021.

[34] S. Zhou, X. Dong, Y. Hua, J. Yu, and Z. Ren, "Predefined formation-containment control of high-order multi-agent systems under communication delays and switching topologies," *IET Control Theory and Applications*, vol. 15, no. 12, pp. 1661–1672, 2021.

[35] J. González-Sierra, M. Ramírez-Neria, J. Santiaguillo-Salinas, and E. G. Hernandez-Martinez, "Saturated formation containment control for a heterogeneous multi-agent system with unknown perturbations," *Automatica*, vol. 159, p. 111 343, 2024.

[36] W. Jiang, G. Wen, Z. Peng, T. Huang, and A. Rahmani, "Fully distributed formation-containment control of heterogeneous linear multiagent systems," *IEEE Transactions on Automatic Control*, vol. 64, no. 9, pp. 3889–3896, 2018.

[37] C. Bi, X. Xu, L. Liu, and G. Feng, "Formation-containment tracking for heterogeneous linear multiagent systems under unbounded distributed transmission delays," *IEEE Transactions on Control of Network Systems*, vol. 10, no. 2, pp. 822–833, 2022.

[38] Y. Lu, X. Dong, Q. Li, J. Lü, and Z. Ren, "Time-varying group formation-containment tracking control for general linear multiagent systems with unknown inputs," *IEEE Transactions on Cybernetics*, vol. 52, no. 10, pp. 11 055–11 067, 2021.

[39] W. Cao, D. Zhang, and G. Feng, "Resilient semi-global finite-time cooperative output regulation of heterogeneous linear multi-agent systems subject to denial-of-service attacks," *Automatica*, vol. 173, p. 112 099, 2025.

[40] X. Jiang, R. Jiao, B. Li, X. Zhang, and H. Yan, "Finite-time consensus of second-order multiagent systems with input saturation via hybrid sliding-mode control," *IEEE Transactions on Automation Science and Engineering*, vol. 22, pp. 14 623–14 632, 2025.

[41] B. An, H. Fan, B. Wang, and L. Liu, "Fully distributed finite-time formation tracking of heterogeneous multi-agent systems under directed networks," *IEEE Transactions on Automation Science and Engineering*, vol. 22, pp. 21 960–21 974, 2025.

[42] Y. Sun, Z. Ji, Y. Shi, and Y. Liu, "Event-based finite time stabilizability and formation control of multi-agent systems," *IEEE Transactions on Automation Science and Engineering*, vol. 22, pp. 7887–7896, 2025.

[43] D. Zhang, H. L. Chen, Q. Lu, C. Deng, and G. Feng, "Finite-time cooperative output regulation of heterogeneous nonlinear multi-agent systems under switching DoS attacks," *Automatica*, vol. 173, p. 112 062, 2025.

[44] A. Polyakov, "Nonlinear feedback design for fixed-time stabilization of linear control systems," *IEEE Transactions on Automatic Control*, vol. 57, no. 8, pp. 2106–2110, 2011.

[45] Y.-H. Su, P. Bhowmick, and A. Lanzon, "A fixed-time formation-containment control scheme for multi-agent systems with motion planning: applications to quadcopter UAVs," *IEEE Transactions on Vehicular Technology*, vol. 73, no. 7, pp. 9495–9507, 2024.

[46] S. Zhou, D. Sun, and G. Feng, "Distributed adaptive fixed-time formation tracking for heterogeneous multi-agent systems," *Automatica*, vol. 183, p. 112 632, 2026.

[47] T. Xu, Z. Duan, Z. Sun, and G. Chen, "Distributed fixed-time coordination control for networked multiple Euler–Lagrange systems," *IEEE Transactions on Cybernetics*, vol. 52, no. 6, pp. 4611–4622, 2022.

[48] Z. Zuo, "Nonsingular fixed-time consensus tracking for second-order multi-agent networks," *Automatica*, vol. 54, pp. 305–309, 2015.

[49] Z. Zuo, B. Tian, M. Defoort, and Z. Ding, "Fixed-time consensus tracking for multi-agent systems with high-order integrator dynamics," *IEEE Transactions on Automatic Control*, vol. 63, no. 2, pp. 563–570, 2017.

[50] W. Cheng, K. Zhang, B. Jiang, and S. X. Ding, "Fixed-time formation tracking for heterogeneous multiagent systems under actuator faults and directed topologies," *IEEE Transactions on Aerospace and Electronic Systems*, vol. 58, no. 4, pp. 3063–3077, 2022.

[51] Y. Cai, H. Zhang, Y. Wang, Z. Gao, and Q. He, "Adaptive bipartite fixed-time time-varying output formation-containment tracking of heterogeneous linear multiagent systems," *IEEE Transactions on Neural Networks and Learning Systems*, vol. 33, no. 9, pp. 4688–4698, 2021.

[52] Z. Qu, *Cooperative control of dynamical systems: applications to autonomous vehicles*. Springer Science and Business Media, 2009.

[53] J. Huang, *Nonlinear output regulation: theory and applications*. Society for Industrial and Applied Mathematics, 2004.

[54] B. Tian, H. Lu, Z. Zuo, and H. Wang, "Fixed-time stabilization of high-order integrator systems with mismatched disturbances," *Nonlinear Dynamics*, vol. 94, pp. 2889–2899, 2018.

[55] P. Wieland, R. Sepulchre, and F. Allgöwer, "An internal model principle is necessary and sufficient for linear output synchronization," *Automatica*, vol. 47, no. 5, pp. 1068–1074, 2011.

[56] X. Dong, Y. Zhou, Z. Ren, and Y. Zhong, "Time-varying formation tracking for second-order multi-agent systems subjected to switching topologies with application to quadrotor formation flying," *IEEE Transactions on Industrial Electronics*, vol. 64, no. 6, pp. 5014–5024, 2016.

[57] G. H. Hardy, J. E. Littlewood, G. Pólya, and G. Pólya, *Inequalities*. Cambridge University Press, 1952.

[58] D. Luenberger, "Canonical forms for linear multivariable systems," *IEEE Transactions on Automatic Control*, vol. 12, no. 3, pp. 290–293, 1967.

[59] M. Basin, Y. Shtessel, and F. Aldukali, "Continuous finite-and fixed-time high-order regulators," *Journal of the Franklin Institute*, vol. 353, no. 18, pp. 5001–5012, 2016.

Shiyu Zhou (Student Member, IEEE) received the B.Eng. degree in automation from Northwestern Polytechnical University, Xi'an, China, in 2019, and the M.Eng. degree in control science and engineering from the Beihang University, Beijing, China, in 2022. She is currently pursuing the Ph.D. degree with the Department of Mechanical Engineering, City University of Hong Kong, Hong Kong.

Her current research interests include cooperative control of multi-agent systems and synchronization of complex networks.

Dong Sun (Fellow, IEEE) received the B.Eng. and M.Eng. degrees in precision instrument and mechanology from Tsinghua University, Beijing, China, in 1990 and 1994, respectively, and the Ph.D. degree in robotics and automation from The Chinese University of Hong Kong, Hong Kong, in 1997. He is a Chair Professor with the Department of Biomedical Engineering, City University of Hong Kong, Hong Kong, SAR, China.

Professor Sun is currently Fellow of the Canadian Academy of Engineering in Canada, Member of the European Academy of Sciences and Arts, Fellow of the International Academy of Medical and Biological Engineering, Fellow of the American Society of Mechanical Engineers.

Xiwang Dong (Senior Member, IEEE) received the B.E. degree in automation from Chongqing University, Chongqing, China, in 2009, and the Ph.D. degree in control science and engineering from Tsinghua University, Beijing, China, in 2014.

From 2014 to 2015, he was a Research Fellow with the School of Electrical and Electronic Engineering, Nanyang Technological University, Singapore, and from 2014 to 2018, he was a Lecturer with the School of Automation Science and Electrical Engineering, Beihang University, Beijing, where he is currently a Professor and the Dean of the Institute of Unmanned System. His research interests include cooperative decision-making, control and guidance of swarm systems.

Prof. Dong was a recipient of the National Natural Science Fund for Excellent Young Scholars in 2019, the first prize of Natural Science Award of Chinese Association of Automation in 2024, the first prize of Technological Invention Award of Chinese Institute of Command and Control in 2024, and the Springer Outstanding Thesis Award in 2015. He serves as the Associate Editor of IEEE Robotics and Automation Letters and Unmanned Systems.

Gang Feng (Fellow, IEEE) received the B.Eng. and M.Eng. degrees in automatic control from Nanjing Aeronautical Institute, Nanjing, China, in 1982 and 1984, respectively, and the Ph.D. degree in electrical engineering from the University of Melbourne, Melbourne, VIC, Australia, in 1992.

From 1992 to 1999, he was a Lecturer/Senior Lecturer with the School of Electrical Engineering, University of New South Wales, Sydney, Australia. Since 2000, he has been with the City University of Hong Kong, Hong Kong, where he is currently a Chair Professor of mechatronic engineering. His current research interests include multiagent systems and control, intelligent systems and control, and networked systems and control.

Prof. Feng was the recipient of the IEEE Computational Intelligence Society Fuzzy Systems Pioneer Award, IEEE Transactions on Fuzzy Systems Outstanding Paper Award, Alexander von Humboldt Fellowship, and the City University of Hong Kong Outstanding Research Award. Since 2016, he has been listed as an SCI highly cited Researcher by Clarivate Analytics. He is with the Advisory Board of Unmanned Systems. He has been an Associate Editor for IEEE TRANSACTIONS ON AUTOMATIC CONTROL, IEEE TRANSACTIONS ON FUZZY SYSTEMS, IEEE TRANSACTIONS ON SYSTEMS, MAN, AND CYBERNETICS, PART C, *Mechatronics*, *Journal of Systems Science and Complexity*, *Autonomous Intelligent Systems*, *Guidance, Navigation and Control*, and *Journal of Control Theory and Applications*.